



TESLA REPORT 2006-01  
DESY THESIS 2006-001

Warsaw University of Technology  
Department of Electronics and Information Technologies  
Institute of Electronic Systems

**Wojciech Jałmużna** (index no 180896)  
Warsaw ELEHP Group and DESY LLRF Team

Thesis for Master of Science in Electronics Engineering

**Design and implementation of universal  
mathematical library supporting  
algorithm development for FPGA based  
systems in high energy physics  
experiments**

The work done under supervision of  
prof. nzw. dr hab. Ryszard Romaniuk and dr Krzysztof Pozniak, in cooperation with dr Stefan Simrock

Warsaw, February 2006

# Contents

I. Abstract.....	3
II. Abstract in Polish .....	4
1. Introduction.....	7
1.1 Control algorithm.....	10
1.2 Modern solutions.....	12
1.3 FPGA based controller ( SIMCON ).....	15
1.4 Algorithm development.....	20
2. System requirements.....	23
3. Concept of a synchronous mathematical library for FPGA chips.....	24
3.1 math_basic_signed and math_basic_unsigned modules.....	26
3.2 math_complex module.....	27
3.3 math_matrix module.....	28
3.4 IQ estimator.....	29
3.5 CORDIC stage.....	30
3.6 Magnitude and Phase detector.....	31
3.7 Sin/Cos calculation.....	32
3.8 SRT stage.....	34
3.9 Fixed point divider.....	37
3.10 Floating point unit.....	37
3.11 OPB wrapper.....	38
3.12 Summary.....	38
4. Implementation.....	40
4.1 math_basic_unsigned.....	40
4.2 math_basic_signed.....	42
4.3 math_complex.....	44
4.4 math_matrix.....	45
4.5 IQ demodulator.....	47
4.6 CORDIC.....	48
4.7 SRT.....	51
4.8 Floating point unit.....	53
4.9 FIR filter.....	55
4.10 OPB wrapper.....	57
4.11 Summary.....	58
5. Tests of designed system.....	59
5.1 Cavity detuning measurement – algorithm and implementation.....	61
5.2 Floating point unit tests.....	72
5.3 Matrix multiplication tests.....	73
6. Summary and conclusions.....	75
References.....	77
Acknowledgments.....	79
7. Appendixes.....	80

# I. Abstract

The X-ray free-electron laser XFEL that is being planned at the DESY research center in cooperation with European partners will produce high-intensity ultra-short X-ray flashes with the properties of laser light. This new light source, which can only be described in terms of superlatives, will open up a whole range of new perspectives for the natural sciences. It could also offer very promising opportunities for industrial users.

SIMCON (**S**IMulator and **C**ONtroller) is the project of the fast, low latency digital controller dedicated for LLRF system in VUV FEL experiment based on modern FPGA chips. It is being developed by ELHEP group in Institute of Electronic Systems at Warsaw University of Technology. The main purpose of the project is to create a controller for stabilizing the vector sum of fields in cavities of one cryomodule in the experiment. The device can be also used as the simulator of the cavity and testbench for other devices. Flexibility and computation power of this device allow implementation of fast mathematical algorithms.

This paper describes the concept, implementation and tests of universal mathematical library for FPGA algorithm implementation. It consists of many useful components such as IQ demodulator, division block, library for complex and floating point operations, etc. It is able to speed up implementation time of many complicated algorithms. Library has already been tested using real accelerator signals and the performance achieved is satisfactory.

## II. Abstract in Polish

Projekt XFEL, który planowany jest w instytucie badawczym DESY w Hamburgu będzie w stanie dostarczyć krótkie impulsy promieniowania X o wysokim natężeniu z właściwościami światła laserowego. Jego świetlnosc może być nawet milion razy większa od najbardziej nowoczesnych źródeł promieniowania X. Międzynarodowa grupa badawcza o nazwie 'TESLA collaboration' testuje obecnie nowatorski technologie w ośrodku DESY. Osiągnęła ona już wiele z kluczowych celów postawionych przed nimi. XFEL umożliwi wykonywanie zaawansowanych badań w Europie. Stworzy również wiele możliwości dla ośrodków przemysłowych. Pilotowym odcinkiem dla XFEL jest akcelerator VUV-FEL, w którym odbywają się testy.

Jedną z nowatorskich technologii wprowadzonych w użycie przy VUV-FELu są programowalne układy FPGA. W ciągu ostatnich lat zaobserwowano szybki rozwój na tym rynku. Obecnie moc obliczeniowa tych układów może być porównana z mocą obliczeniową procesorów DSP. Ponadto architektura tych chipów jest otwarta – może być optymalizowana razem z algorytmem matematycznym. Wiele układów FPGA ma możliwość użycia procesorów osadzonych takich jak PowerPC, Nios, Microblaze. Programy pisane na te procesory mogą zostać połączone ze sprzętowymi blokami równoległego przetwarzania sygnału.

W chwili obecnej w użyciu znajduje się oparty na układzie FPGA kontroler opracowany przez grupę ELHEP. Jest to kolejna generacja płyty z rodziny SIMCON. Bazuje ona na chipie FPGA XC2VP30 firmy Xilinx. Bogate peryferia oferują duże możliwości komunikacyjno-obliczeniowe. Może ona stać się bazą wielu implementacji algorytmów matematycznych.

Szybki rozwój możliwości technicznych pociąga za sobą rozwój algorytmów matematycznych. Ich implementacja przy użyciu języka opisu sprzętu ( VHDL ) staje się skomplikowana i czasochłonna. Rośnie czas dostarczenia gotowego produktu. Na wprost tego wychodzą producenci oprogramowania używanego do implementacji. Interfejsy tych programów są coraz bardziej uproszczone. Oferują one graficzne narzędzia do tworzenia opisów sprzętu. Przyspiesza to znacznie proces implementacji.

Pociąga za sobą również jedną wadę – maleje kontrola nad szczegółami implementacji w sprzęcie. Praca ta prezentuje inne z możliwych rozwiązań tego problemu. Jej celem jest stworzenie koncepcji oraz implementacja uniwersalnej i parametrycznej biblioteki matematycznej wspierającej implementację i rozwój algorytmów matematycznych w układach FPGA.

Biblioteka została podzielona na następujące części:

- moduły wejściowe  
w skład tej grupy wchodzi moduły takie jak demodulator IQ oraz blok obliczający amplitudę i fazę liczby zespolonej. Użyte mogą zostać do wstępnej konwersji sygnału z akceleratora do wymaganej reprezentacji. Dostarczają one sygnał do komponentów z kolejnej grupy.
- moduły obliczeniowe  
są to główne moduły wykonujące konkretne obliczenia matematyczne. W ich skład wchodzi bloki takie jak: dzielenie stało pozycyjne, obliczanie funkcji trygonometrycznych, operatory operacji na liczbach zespolonych, macierzowe operacje arytmetyczne, regulowane filtry oraz jednostka do obliczeń zmiennie pozycyjnych.
- wsparcie dla systemów osadzonych  
w tej grupie znajduje się moduł 'OPB wrapper' mapujący zbiór rejestrów zdefiniowanych w strukturze FPGA w przestrzeń adresową systemu osadzonego. Umożliwia to mieszane podejście do implementacji algorytmów – mniej krytyczne części mogą zostać zaimplementowane w języku wyższego poziomu ( na przykład C ) i komunikować się z krytycznymi sekcjami obliczanymi przez sprzęt. Moduł ten umożliwia również dołączenie wymienionej wyżej jednostki zmiennopozycyjnej jako koprocesora dla PowerPC.
- moduły niskopoziomowe

są to biblioteki podstawowe użyte do zaimplementowania pozostałych modułów. Udostępnione są one użytkownikowi, aby mógł użyć je w przypadku kiedy wymagana jest funkcjonalność nieuwzględniona w bibliotece. Implementują one podstawowe koncepty operacji arytmetycznych takie jak arytmetyka naszycona, operatory arytmetyczne dla macierzy, liczb zespolonych, liczb zmiennopozycyjnych.

Architektura bibliotek jest otwarta. Dzięki temu istnieje wiele możliwości dodawania nowych komponentów i ulepszania starych. Nowe komponenty mogą zostać dodane do biblioteki nawet przez zwykłych użytkowników. Wszystkie bloki zostały zoptymalizowane aby zapewnić rozsądny wybór między użytymi zasobami a szybkością działania. Jednak w miarę rozwoju rynku FPGA – rosnących możliwości technicznych – konieczne będzie dostosowywanie biblioteki do zmieniających się warunków.

Wszystkie użyte w niej algorytmy obliczeniowe są algorytmami dobrze znanymi w przetwarzaniu DSP. Przykładem może być tu algorytm demodulacji IQ używany obecnie w kontrolerze FPGA dla moduły ACC1 akceleratora VUV-FEL lub algorytm dzielenia SRT używany w procesorach firmy Intel.

Szczegóły implementacji – interfejsy i parametry - poszczególnych modułów pokazane zostały w rozdziale 4 tej pracy.

Rozdział 5 przedstawia testy biblioteki w środowisku akceleratorowym. W tym celu zaimplementowany został algorytm matematyczny pomiaru odstrojenia wnęki rezonansowej podczas pojedynczego pulsu pola elektromagnetycznego wewnątrz wnęki. Uzyskana implementacja spełnia wszystkie oczekiwania – wejdzie ona w skład planowanego systemu kontroli. Przetestowany został również blok operacji zmiennopozycyjnych. Przyspieszenie obliczeń procesora osadzonego w porównaniu z emulacją programową wynosi około 1000%. Rezultaty uzyskane dla mnożenia macierzy 20 na 20 elementów również są bardzo ciekawe. Czas wykonania takiego mnożenia wynosi około 80 us.

Przedstawiona biblioteka spełnia wszystkie wymagania postawione przez system sterowania LLRF i ma szansę stać się popularnym narzędziem implementacji algorytmów matematycznych.

# 1. Introduction

The X-Ray Free-Electron Laser, which is planned at the DESY research center [15] will produce high-intensity ultra-short X-ray pulses with the properties of laser light. At peak values, its brilliance is a billion times higher than that of the most modern X-ray light sources, and its average brilliance is 10 000 times higher. An international research team, the TESLA collaboration, is currently demonstrating the facility's pioneering technology at the DESY research center in Hamburg. It has already achieved the key milestones it has been aiming for. The free-electron X-ray laser will make it possible to do leading-edge research in Europe and will also offer very promising opportunities for industrial users

The layout of the accelerator and laser facility is shown on Figure 1.

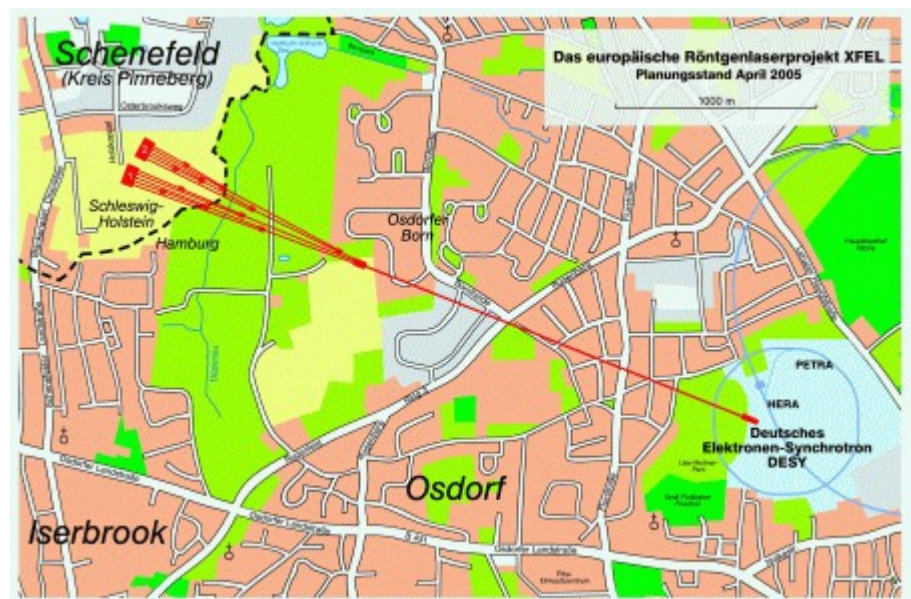


Figure 1: X-FEL facility layout

Main parameters of XFEL facility are [15]:

Total length of the facility	approx. 3.4 km
Accelerator tunnel	approx. 2.1 km
Depth underground	6 - 38 m
Experimental hall	10 experimental stations at 5 beamlines,
Scope for expansion	Second hall with an 10 experimental stations
Wavelength of X-ray radiation	6 to 0.085 nanometers (nm)
Length of radiation pulses	below 100 femtoseconds (fs)

*Table 1: X-FEL main parameters*

The planned facility will include a superconducting linear accelerator that brings tightly bundled “bunches” of electrons to energies of several billion electron volts. At that point, the electrons race at almost the speed of light along a slalom course through a special arrangement of magnets called the “undulator.” As they go, they emit X-ray radiation that amplifies itself during the flight. The results are brilliant: Extremely short and intense X-ray flashes with laser properties. For such an X-ray laser to work, an electron beam of extremely high quality is required. And the TESLA superconducting accelerator technology is already making it possible to generate this kind of electron beam today.

Before the electrons can emit X-ray flashes, they must first be accelerated to energies of several billion electronvolts. That's exactly what happens inside the resonators, where electromagnetic fields accelerate the particles. The resonators are made of niobium and are superconducting: When they are cooled to a temperature of -271 °C, they lose their electrical resistance. Electrical current then flows through the resonators with almost no losses whatsoever - and that's an extremely efficient and energy-saving method of acceleration. Nearly the entire rf power is transferred to the particles. Moreover, the superconducting resonators deliver an extraordinarily fine and even electron beam of extremely high quality. In the X-ray laser, each of several billion electrons needs to have the same energy and direction. They also need to be combined into bunches with a diameter of no more than one tenth of a millimeter to achieve the necessary peak current of 5kA. Unless the electron beam meets these very special

requirements, the X-ray laser does not work.

The new free-electron laser VUV-FEL - the pilot facility for the XFEL - , which generates vacuum ultraviolet (VUV) and soft X-ray radiation in a range down to wavelengths of six nanometers, was commissioned in 2004, making possible groundbreaking experiments. To accommodate the new free-electron laser, the 100-meter-long TESLA test facility was modified to a total length of 260 meters and extended to the VUV-FEL. Both VUV-FEL and XFEL are based on the same superconducting technology.

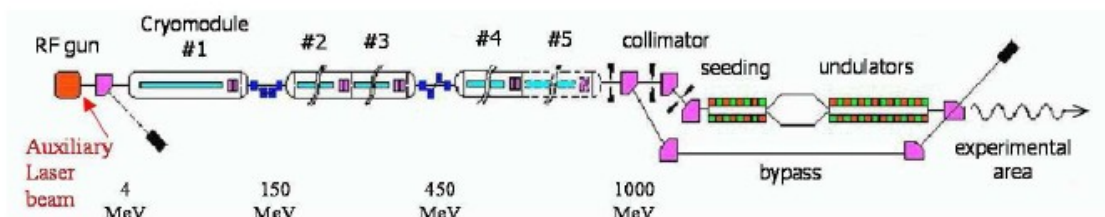


Figure 2: VUV-FEL structure schematic

In the VUV-FEL cavities are grouped into cryomodules which contain 8 cavities each. The cavities are powered by klystrons ( 32 per klystron ). In order to get appropriate beam acceleration two conditions must be met:

1. the electromagnetic field inside resonators must be stabilized ( to ensure stable beam energy )
2. it must have appropriate phase ( for bunch compression and acceleration )

The regulation of the field is performed by the LLRF – Low Level Radio Frequency control system. It controls I and Q components of resonator field. They correspond to real and imaginary part of the field vector. The control section, powered by one klystron, may consist of many cavities, so the LLRF system is used to control vector sum of up to 32 cavity fields. The system consists of many devices such as: downconverters, digital feedback controllers, vector modulators, piezo controllers, timing modules, and many ADC boards for monitoring the signals in the system.

## 1.1 Control algorithm

The main control loop in the LLRF system starts at the cavity probe. The signals (1.3GHz) are downconverted to an intermediate frequency of 250KHz. Eight downconverted signals are connected to inputs of digital controller. It samples the probe signal with a frequency of 1MHz. Inside the controller (currently it is a DSP based system) after initial calibration (scaling and leveling), the digital processing is performed in I/Q detector applying the signal  $v_m$  of the intermediate frequency at 250 kHz. The resultant cavity voltage envelope (I, Q) is calibrated, so to compensate the phase offset for an individual measurement channel. The vector sum of up to 32 signals is needed for the actual control processing. Feedforward and Feedback algorithms can be used to control the system.

The Set-Point table delivers the required signal level, which is compared to the actual average value of the cavities voltage envelope. Then the proportional controller amplifies the signal error according to data from the GAIN table and closes the feedback loop. Additionally the Feed-Forward Table is applied to improve compensation of the repetitive perturbations induced by the beam loading and by the dynamic Lorentz force detuning. I and Q signals are produced to drive the klystron. These two signals are used by the vector modulator to reconstruct the complex signal. The output of this vector modulator drives the klystron. When using 1MHz sampling rate, the probe samples are updated every  $1\mu s$ . High gain must be used to stabilize the field using feedback algorithm. This may cause instability in the system if the feedback latency is too high. The maximum latency for the feedback algorithm has been estimated to about  $1\mu s$  (for the whole control loop including latency of system and controller board). The estimated system delay is about 500ns. It means that maximum delay of the controller can not exceed 500ns. The requirements for the stability of the amplitude and phase of the field are tight: for the amplitude  $3 \cdot 10^{-4}$  and for the phase 0.1 degree. The main problem is noise which comes from microphonics, Lorentz force detuning and beam loading. In addition lots of elements in the control loop are nonlinear, for example klystron, vector modulator or preamplifiers. Every conversion from analog to digital signal adds noise to the system. Moreover the temperature changes cause phase drifts in

cables. All these distortion are added to the control signal and force the controller to compensate using sophisticated algorithms. This requires a big computation power of the controller and wide data throughput.

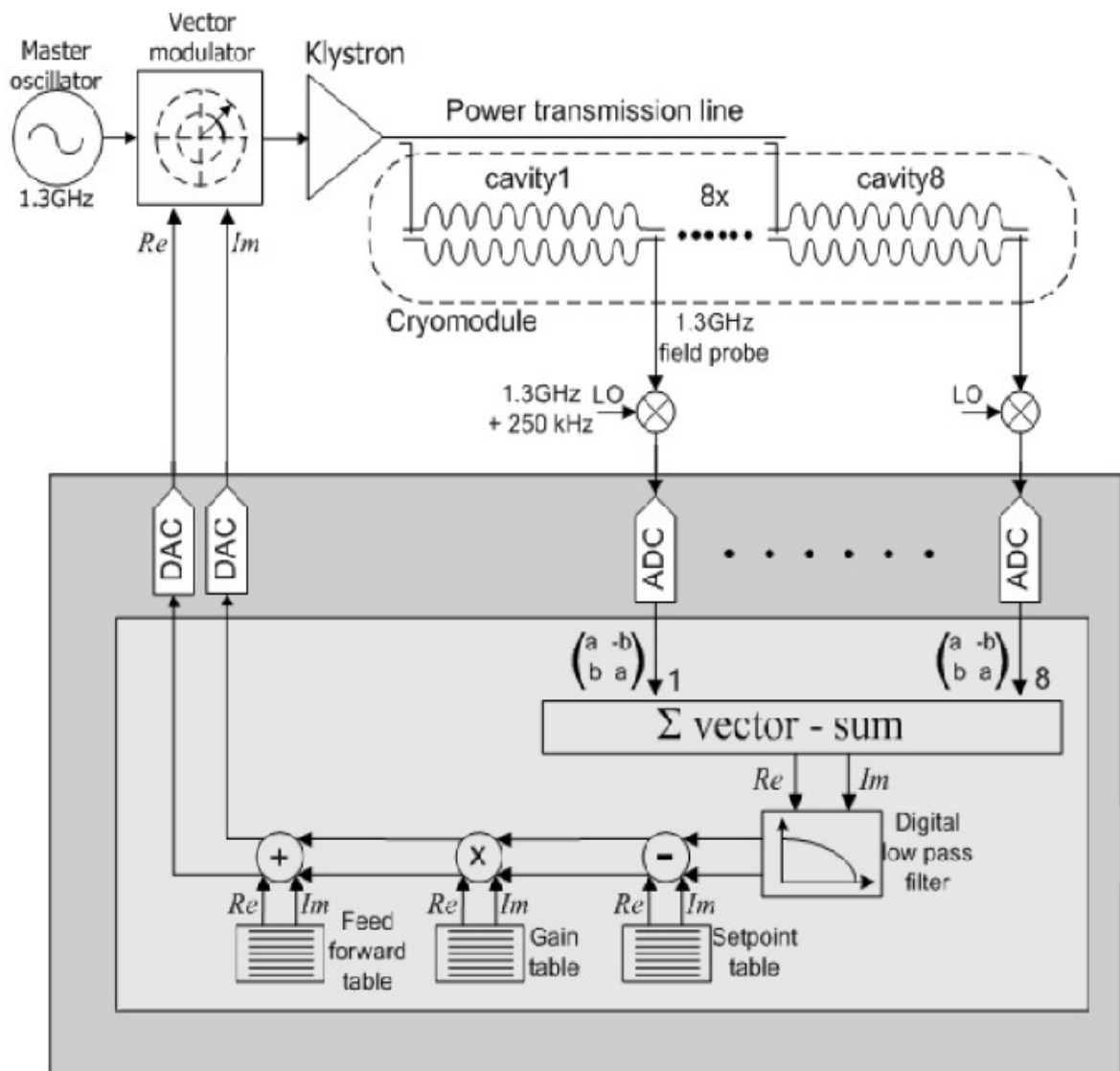


Figure 3: Control system schematic

The current solution is based on the system with DSP processor (TMS320C67 from Texas Instruments). The controller is divided into three boards - ADC board with 14-bit analog to digital converters sampling with a frequency of 1MHz, the DSP board with TMS320C67 processors and DAC board (14 bit, 1MHz). All the boards are connected to each other using gigalink interface. Actual computation power is close to the limit, the algorithm is performed in a time longer than  $1\mu s$ . Moreover, during last months there are additional needs for some new features. The only way to extend current system with new features is to add more DSP processors. This solution requires integration of new DSP board into existing system. It may cause some additional problems and delays in machine operations.

To increase computation power and the delay of LLRF control system, both the algorithm and hardware must be optimized. Unfortunately DSP processors have fixed architecture so only the software can be processed. This will not grant the flexibility required for further system development.

## **1.2 Modern solutions**

During past years very fast progress on the FPGA market was observed. Nowadays FPGA chips have reached computation power that can be compared with DSP processors. Moreover the architecture of those chips is not fixed. Just like software algorithm it can be optimized to achieve optimal speed or resources usage ( depends on requirements ). FPGA chips offer variety of the embedded solutions such as PowerPC, Microblaze, Nios which can be easily used in addition to fast, parallel signal processing.

Typical low level architecture of FPGA chip is shown on Figure 4

It consists of an array of logic blocks and routing channels. Multiple I/O pads may fit into the height of one row or the width of one column. Generally, all the routing channels have the same width. A logic block consists of a LookUp Table with 4 inputs and a FlipFlop as shown on Figure 5.

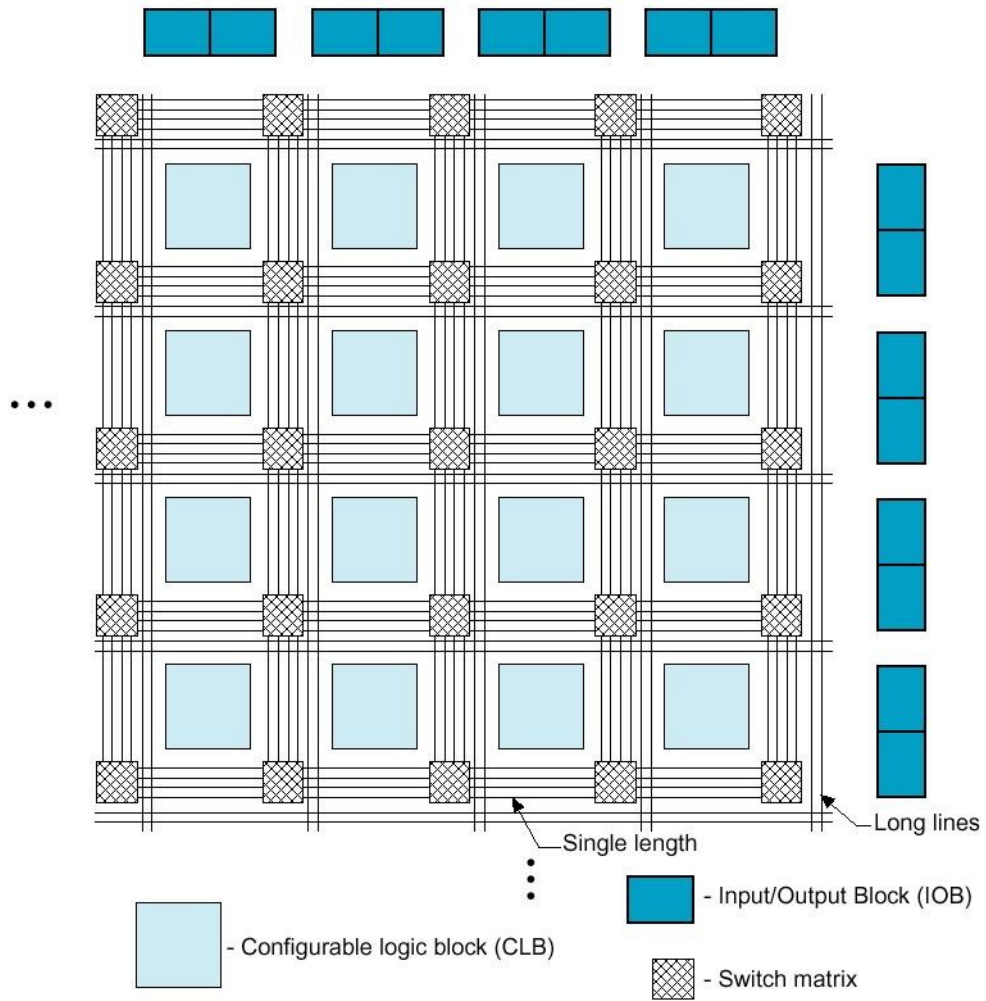


Figure 4: Low level architecture of FPGA chip

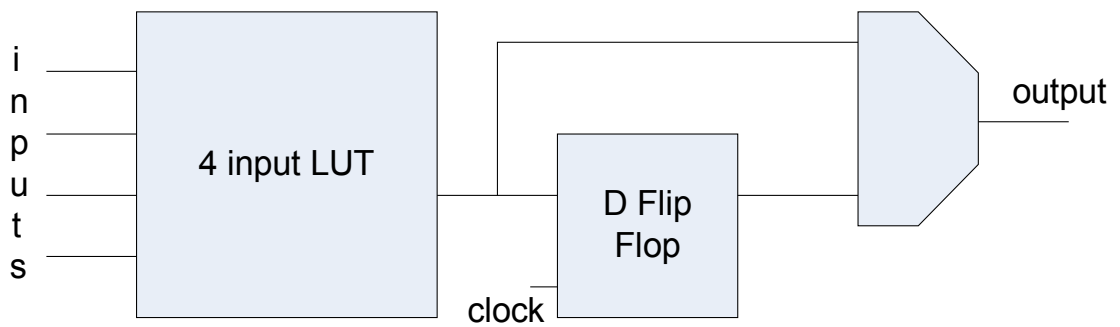


Figure 5: Logic block structure

In the modern solutions there are many functional blocks embedded into the chip's architecture. These functional blocks are:

- RAM memory which can be used in data acquisition process

- dedicated DSP blocks for arithmetic operations
- digital clock managers ( PLLs ) for clock conversions
- Gigabit serializers that can connected to optical transceivers
- embedded processors which can run higher level software

Usage of these block simplifies the structure required for the algorithms, reduces delays and increases computation power. Moreover each of these blocks can be used in parallel.

The block RAM memory resources embedded into Xilinx FPGA [17] chips such as Virtex 2 are 18 Kb of true Dual-Port RAM, programmable from 16K x 1 bit to 512 x 36 bit, in various depth and width configurations. Each port is totally synchronous and independent, offering three "read-during-write" modes. Block RAM memory is cascadable to implement large embedded storage blocks. Supported memory configurations for dual-port and single-port modes are shown in Table 2.

<b>16K x 1 bit</b>	<b>4K x 4 bits</b>	<b>1K x 18 bits</b>
<b>8K x 2 bits</b>	<b>2K x 9 bits</b>	<b>512 x 36 bits</b>

*Table 2: internal memory configurations*

A multiplier block is associated with each RAM memory block. The multiplier block is a dedicated 18 x 18-bit 2s complement signed multiplier, and is optimized for operations based on the block RAM content on one port. The 18 x 18 multiplier can be used independently of the block RAM resource. Read/multiply/accumulate operations and DSP filter structures are extremely efficient.

Both the RAM memory and the multiplier resource are connected to four switch matrices to access the general routing resources.

Processors embedded into FPGA chips have become very popular during past years. The main vendors of embedded solutions are Altera and Xilinx companies [17,18]. Altera introduced Nios and Nios II soft processor core which is built using user logic during configuration process. The similar solution comes from Xilinx company and is called Microblaze. Both companies made a big effort to optimize their cores to achieve high performance. These cores can easily be integrated with other user logic

and peripherals, therefore the hardware implementation of an algorithm can be supported by calculations described in higher level programming language such as C or C++.

The most important and unique embedded solution was introduced by Xilinx company. It is PowerPC 405 hardware core placed directly into silicon structure of FPGA chip. The main advantages of such approach are:

- user logic can be completely independent from processor
- it uses minimal number of FPGA resources
- it offers superior performance in comparison with soft cores

The most known FPGA vendors are Altera and Xilinx companies. Comparison of different chips is shown in Table 3.

<i><b>FPGA chip</b></i>	<i><b>Logic cells</b></i>	<i><b>RAM</b></i>	<i><b>Hardware multipliers</b></i>	<i><b>gigalinks</b></i>	<i><b>PowerPCs</b></i>	<i><b>Max user IO</b></i>
XC2V3000	32,256	1,728	96	0	0	720
XC2V400	51,840	2,160	120	0	0	912
XC2VP30	30,816	2,448	136	8	2	644
XC2VP50	53,136	4,176	232	16	2	852
EP1S30	32,470	3,317	96	0	0	726
EP1SGX40	41,250	3,423	112	20	0	624

*Table 3: parameters of Xilinx and Altera chips*

Although DSP processors are more flexible for complex algorithms, the structural flexibility of FPGA chips together with parallel calculations and integrated peripherals make more powerful unit for general purpose and arithmetic operations. LLRF control system based on FPGAs can be smaller, faster and more extensible than DSP based one.

### **1.3 FPGA based controller ( SIMCON )**

SIMCON (SIMulator and CONtroller) [2,5] is the project of the fast, low latency

digital controller dedicated for LLRF system in VUV FEL experiment. It is being developed by ELHEP group in Institute of Electronic Systems at Warsaw University of Technology. The purpose of the project is to create a controller that can stabilize the vector sum of fields in resonators driven by one klystron and gather experience and knowledge for future XFEL control system development. It can also be used as the simulator of the cavity, test bench for other devices and algorithm development studio. SIMCON design is based on FPGA technology. It allows to create fast hardware devices inside the chip, each dedicated for the particular purpose. Therefore it is faster than currently used controller based on DSP processors. Moreover the flexibility of FPGA chips allows to extend existing controllers with new features without any changes in current implementation and architecture of the PCBs. FPGA technology offers integrated peripherals for the fast communication (optical links) and calculations (embedded PPC or DSP blocks). All these features create powerful platform for control system development. The flexibility of FPGA technology used in SIMCON makes this device multipurpose system which can perform many sophisticated algorithms. Its capabilities are limited by the board architecture which includes size of the FPGA chip used. The basic structure of the SIMCON system is shown on Figure 6.

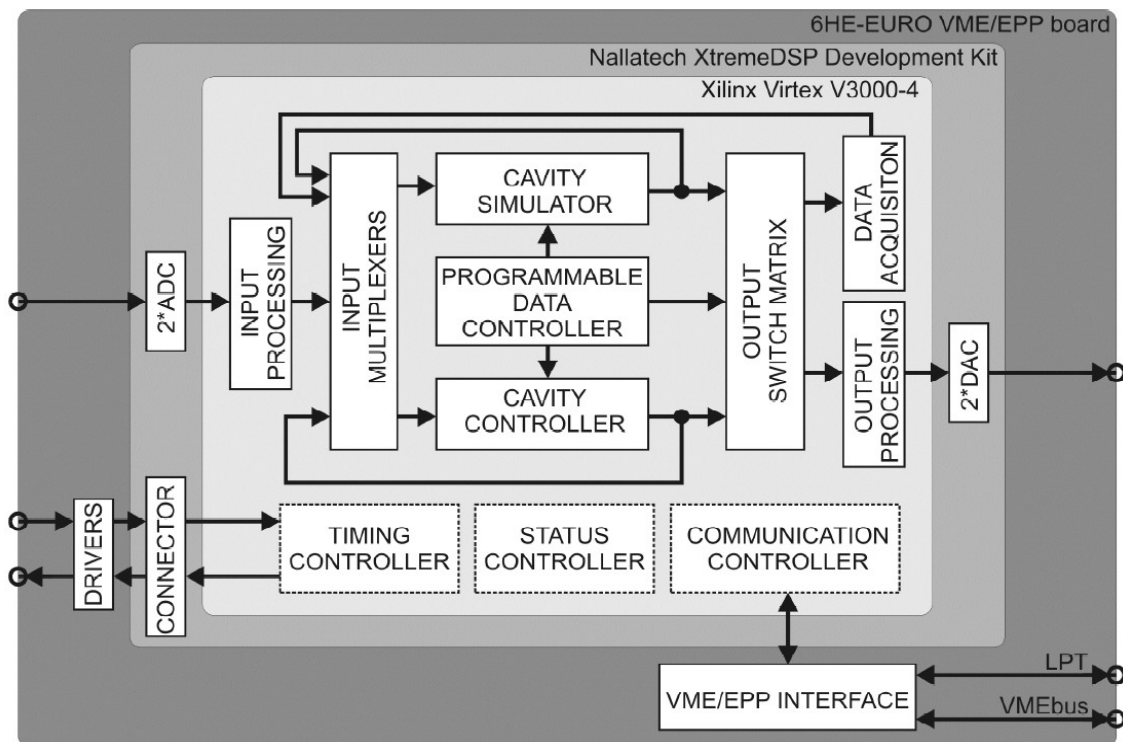
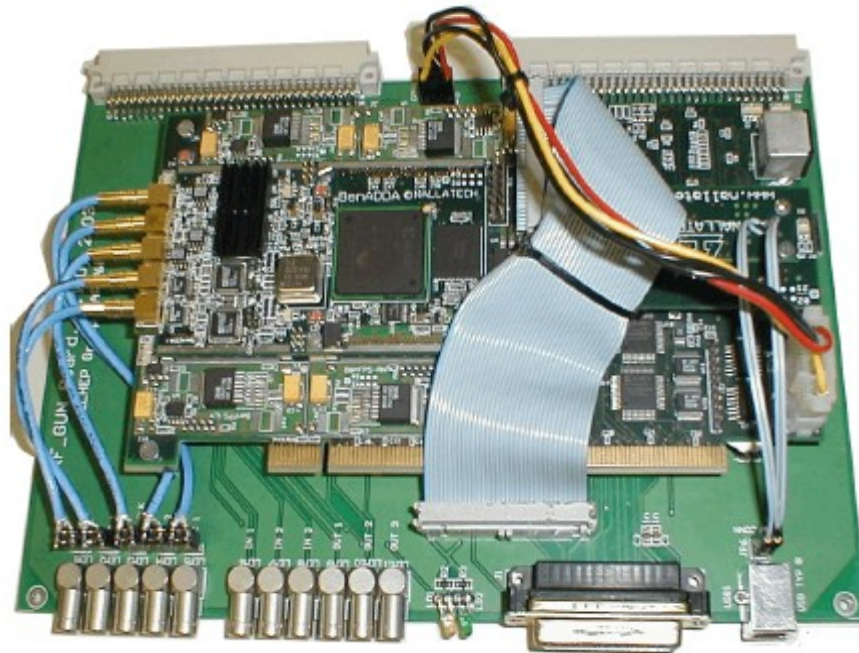


Figure 6: Structure of FPGA based controller

SIMCON family consists of many different boards with different possibilities:

- SIMCON 2.1

two channel version of the controller, two subversions are available – with VME interface and EPP interface. It was mainly used to control a single cavity ( for example test in the CHECHIA module )



*Figure 7: SIMCON 2.1 board*

- SIMCON 3.0

eight channel version of the controller, this board is mainly used to control the vector sum of eight cavities ( most test were done in the ACC1 module of the VUV-FEL accelerator )

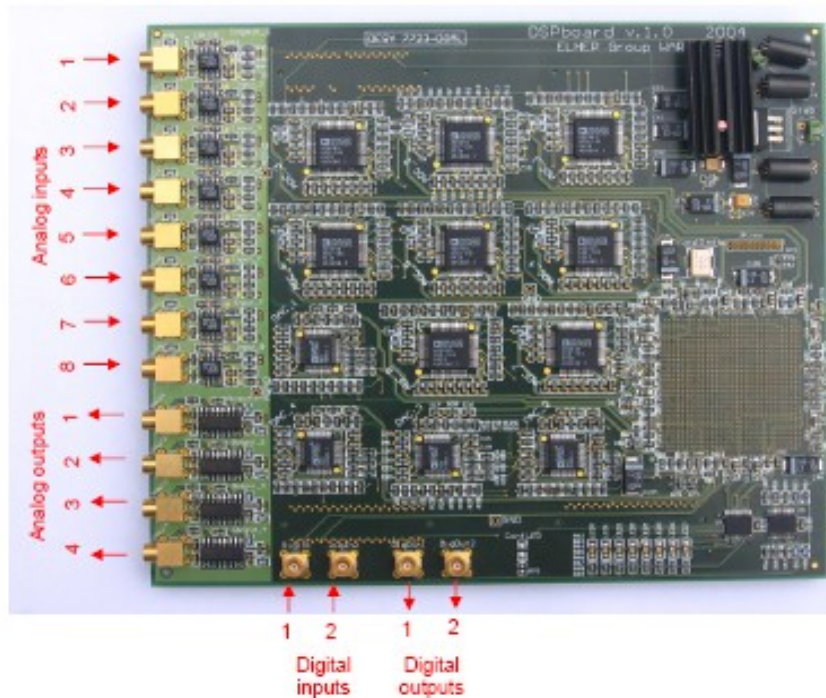


Figure 8: SIMCON 3.0 board

The current version of SIMCON (3.1) was designed for controlling the vector sum of fields in one cryo-module (8 cavities). The main features of the board are:

- Xilinx Virtex II Pro FPGA chip.
- Ten 14-bit ADCs (up to 105 Msp/s) and four 14-bit DACs (up to 160Msp/s).
- 2 inputs for external clock and trigger signals
- 2 outputs for providing the clock and trigger signal
- Additional digital inputs and outputs
- 16MB of SDRAM for embedded system use
- 8MB of SRAM for FPGA use
- Ethernet connector
- 2 Gigabit optical channels
- VME interface



Figure 9: SIMCON 3.1 board

Table 4 presents parameters of SIMCON boards.

	<i>Simcon 2.1</i>	<i>Simcon 3.0</i>	<i>Simcon 3.1</i>
FPGA chip	Virtex II 3000	Virtex II 4000	Virtex 2 Pro 50
ADC channels	1	8	10
DAC channels	2	4	4
Digital Outputs	2	2	2
Digital Inputs	2	2	2
Optical links	-	-	2
PPC	-	-	2
Interface	EPP/VME	VME/ETH/RS232	VME/ETH/RS232

Table 4: SIMCON family parameters

## 1.4 Algorithm development

Powerful FPGA platform such as the SIMCON 3.1 board opens a new possibilities for algorithm development. In the DSP processor, the user has fixed architecture and decides about its functionality and program flow using higher level programming language. Therefore DSP is easier to program than FPGA chips. Unfortunately it is only capable of serial processing with very limited parallel possibilities. On the other hand FPGA chips are dedicated for parallel processing. In FPGA, architecture of the chip must be described using hardware description language such as VHDL ( Very-High-Speed Integrated Circuit Hardware Description Language ), Verilog etc. User decides which calculations are going to be performed in parallel and in serial, which functional blocks and peripherals to use. Program flow control is achieved by defining state machines. Then, if necessary, the user must integrate described structure with embedded processor and create higher level software.

The described process is much more complicated than traditional DSP programming and requires a lot of knowledge about binary operations, FPGA structure and logical systems. Therefore algorithm development for FPGA chips may take much more time than for DSP processors. To overcome this flaw different vendors of FPGA chips and external companies have proposed many software solutions which enable rapid algorithm development.

This software can be splitted into following categories:

- schematic tools
- IP cores

Schematic tools allow programmer to describe even complicated system structures using a simple graphical interface. The system is built using closed functional blocks connected with each other. Then the VHDL code or netlist file is generated. Most advanced schematic tools such as Xilinx System Generator offer high level mathematical operations and integration with popular algorithm development software. These tools give an easy way to describe functionality of the FPGA system, but it is almost impossible to control the hardware architecture of the code. Nowadays, all the design software provided by the manufacturers includes schematic tools for program development.

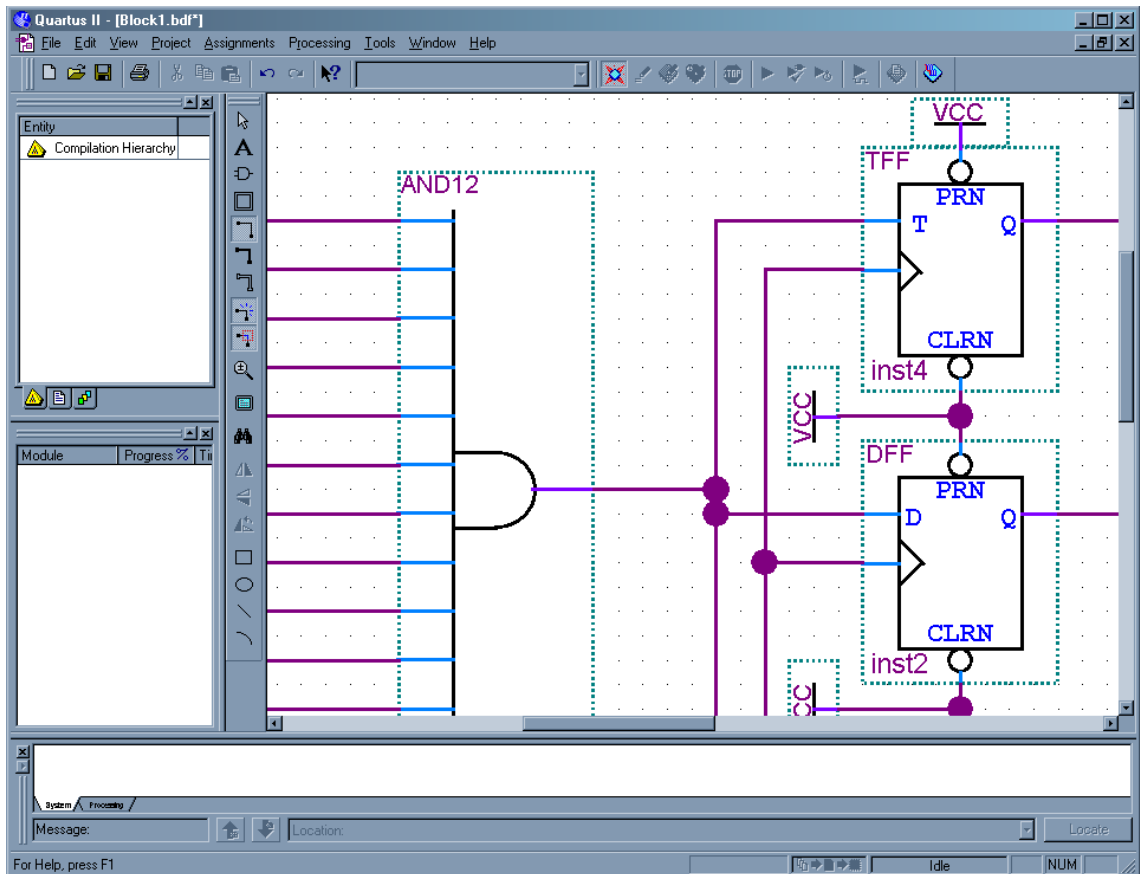


Figure 10: Altera Quartus II schematic tool

The second category are IP cores. These are specialized functional block prepared in a form of netlist or VHDL code which can be included and used in a user program. Usage of IP cores gives an ability to describe the whole system using the VHDL code without need to describe complicated mathematical operations etc. These solution gives better control over FPGA resources and architecture. Unfortunately IP cores are highly specialized and usually patented so there is practically no influence on the interior of blocks – no user modification can be made therefore only small control over their functionality is possible.

Both solutions can be combined – implemented algorithm may be the result of using schematic tool together with VHDL programming and IP cores. Unfortunately these solutions are quite expensive. Moreover LLRF control system requires some functional blocks that are not commonly used, therefore they are not available as IP cores. An excellent example of a combined solution is the Xilinx Embedded Development Kit which allows to build embedded system using a graphical schematic

tool to add IP cores as system's peripherals.

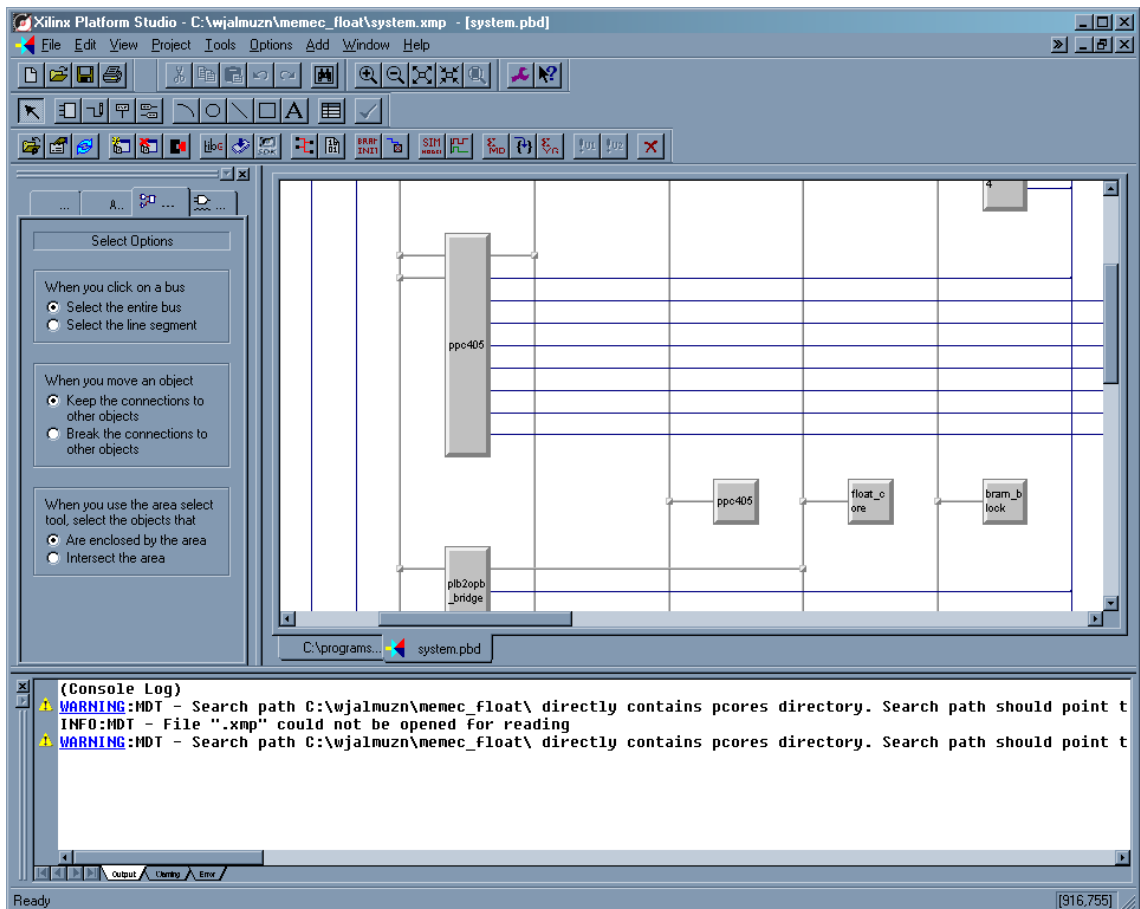


Figure 11: Xilinx EDK for embedded systems

Algorithm development for the LLRF control system requires more flexibility than one offered by described tools. Programming should be done using VHDL language in addition with flexible IP cores and low level libraries developed for this system. The source of the IP cores and libraries should be open to allow users to extend them when needed or modify existing ones according to the needs.

## 2. System requirements

Fast development of electronic systems causes the parallel development of many different mathematical algorithms. FPGAs possibilities are constantly expanding, therefore the structural complexity of hardware is also rising. More work, time and skill is required for algorithm implementation and usage. The aim of this thesis is:

- to design and implement universal mathematical library supporting algorithm development for FPGA based systems in accelerator subsystem design

The main requirements for the project are:

1. the components must be synchronous – maximum working frequency is rising, it is important to have extended control over all delays. It is hard to achieve in asynchronous systems. Moreover it allows to synchronize many independent channels ( for example 8 for SIMCON 3.1 ) and different components.
2. pipelining – it increases the maximum frequency and system bandwidth. The signal samples can be gathered and processed without need to wait for the end of the previous calculations. This speeds up algorithm execution time.
3. flexibility - components can work on many different boards with many FPGA chips and variable channel number and can be modified to fit to particular user needs.
4. choice between speed and resource usage - it allows to use components even when hardware resources are critical, but speed is less important. This approach causes that this library can be used in many offline measurement algorithms with low resource usage
5. platform independence
6. support for popular VHDL synthesizers
7. easy to use
8. easy to maintain and change code

### **3. Concept of a synchronous mathematical library for FPGA chips**

The concept of the library is based on the hierarchical tree of components. The library must fulfill all the requirements for LLRF control system algorithm development. Synchronous mathematical library allows easy latency control versus hardware resources used. Each component is meant to be compatible with existing solutions ( if available ). Moreover functional components are completely hermetical and can be used separately ( providing that libraries in the same tree branch are available), and most important, can be used in any combination of serial and parallel connections.

Most signals from the accelerator modules come as vectors in IQ representation. Therefore the first module in almost every algorithm for this system will be IQ demodulator which converts raw data sampled from ADC to a complex representation. A good example is SIMCON controller algorithm in which the processing starts using such block. This functional block should be included in this library to allow use in other algorithms. After demodulation, the complex signals are calibrated ( scaled, rotated ). It means that arithmetical operations on complex numbers are made. This task is performed by the complex operation module. In some cases signals are filtered. That is why the programmable digital finite impulse response filter was implemented. Both modules can be used in the SIMCON algorithm and many others for rotation matrix multiplication and signal filtering. In some algorithms it is necessary to obtain additional informations about the signal ( for example the magnitude of complex vector or its phase – it was done in Cavity Detuning measurement algorithm ). For this reason a module for magnitude and phase calculation has become part of this library. The algorithm used in this module can be also used to calculate functions such as sine and cosine when latency is not critical.

The only basic arithmetical operation without hardware support in FPGA is the division. Lack of this operation can be major problem in some cases ( for example it is needed in the Cavity Detuning measurement algorithm). Therefore division block is

included in this library.

To extend the flexibility of this library, in addition to fixed point arithmetics, floating point units were added. This feature is valuable especially in connection with embedded system development.

Moreover a special wrapper for the PowerPC embedded processor was added. It allows to connect every component included in this library to Onboard Peripheral Bus (OPB) [17]. This approach allows to combine the algorithm development process between low level hardware description and higher level C programs executed on embedded system.

The tree of components is shown on the Figure 12.

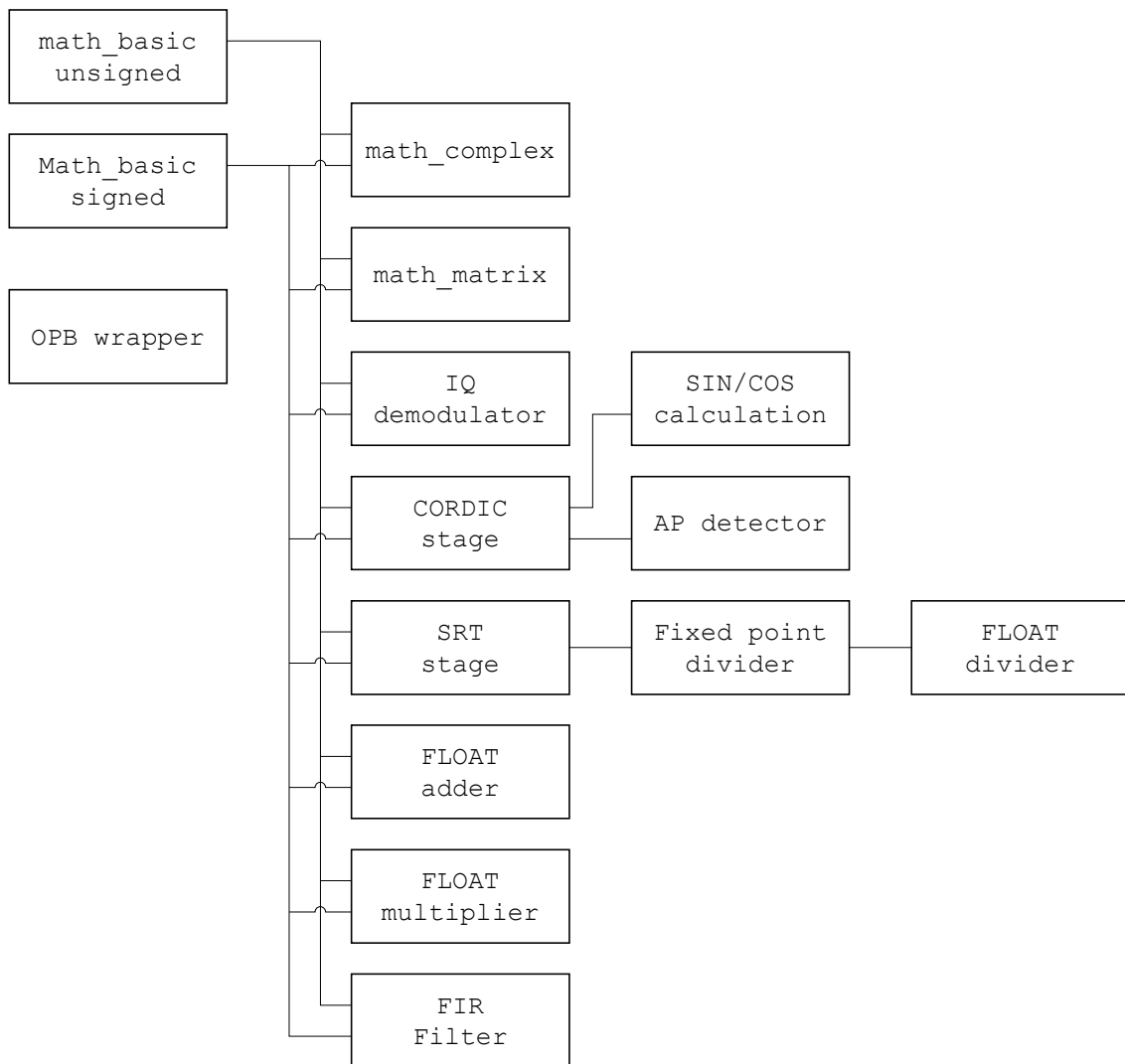


Figure 12: Structure of designed library

### 3.1 math\_basic\_signed and math\_basic\_unsigned modules

These modules provide basic functions for arithmetical operations used in other modules. They are optimized to use dedicate hardware resources embedded into a FPGA array such as hardware multipliers. Functions are meant to be easily used in user applications – their interface is minimal.

The Math\_basic\_signed library provides functions that can operate on signed values using two's complement representation, which is the most popular and intuitive method of representing negative integers. In the two's complement representation, the most significant bit of a signed binary numeral indicates the sign. To obtain the absolute value of the negative number, all the bits are inverted then 1 is added to the result. As one can notice '0' value has only one representation ( no negative '0' and problems associated with it ). Moreover all arithmetic operations are simple binary operations. The library defines functions for number multiplication, addition and subtraction. Moreover it allows to calculate absolute value and negation of a number. There are functions that allow to resize a value to a specified number of bits and to shift it left or right by specified number of bits. Each function has an intuitive interface and can be easily used.

The Math\_basic\_unsigned library provides similar functions that can operate on unsigned binary numbers. As signed library it defines functions for multiplication, addition and subtraction of unsigned binary numbers. Functions for shifting and resizing binary vectors are also included.

In the real time arithmetic operations, overflow is a big problem. When the big values overflow, they suddenly become small or negative. It may lead the whole system to undefined states. Such a situation is not allowed, it can be dangerous for the accelerator and electronic hardware. Therefore, arithmetic operations in both libraries use so called saturation arithmetic. Saturation arithmetic is a version of arithmetic in which all operations such as addition and multiplication are limited to a fixed range between a minimum and maximum value. If the result of an operation is above the maximum it is set to the maximum, while if it is below the minimum it is set to the minimum. In this case, the minimum and maximum values are defined by the length of vectors used to represent numbers.

## 3.2 math\_complex module

This module includes functions needed for complex number operations. It allows to multiply, add and subtract complex numbers represented as real and imaginary parts. Moreover it allows to calculate conjugation and rotate the number by 180 degrees. When resizing complex number, both real and imaginary parts are resized to required number of bits. The base for this module is math\_signed library.

Arithmetic operations on complex number are more complicated than operations on normal numbers. Addition ( or subtraction) of two numbers requires two additions of signed values.

$$z1 = a+jb$$

$$z2 = c+jd$$

The result of an addition is

$$z1+z2 = (a+c) + j(b+d)$$

The result of a multiplication is

$$z1*z2 = (a*c - b*d) + j(a*d + b*c)$$

As one can see multiplication of two complex numbers uses six binary operations ( 4 multiplications and 2 additions/subtractions ). It will take 4 hardware multipliers.

### 3.3 math\_matrix module

This module defines basic components for matrix operations such as addition, subtraction and multiplication. Matrix operations are simple arithmetic operations. The only problem is an amount of data to be processed. Simple 4 by 4 matrix addition requires 16 binary additions. Multiplication of such matrix requires 64 multiplications and 48 additions of binary numbers. This takes a big amount of time when done in series. Each component in this library can be used to calculate one or more matrix elements, therefore calculations can be made in parallel. It reduces the time, but increases the number of FPGA resources used.

Proposed structure for matrix multiplication is shown on Figure 12.

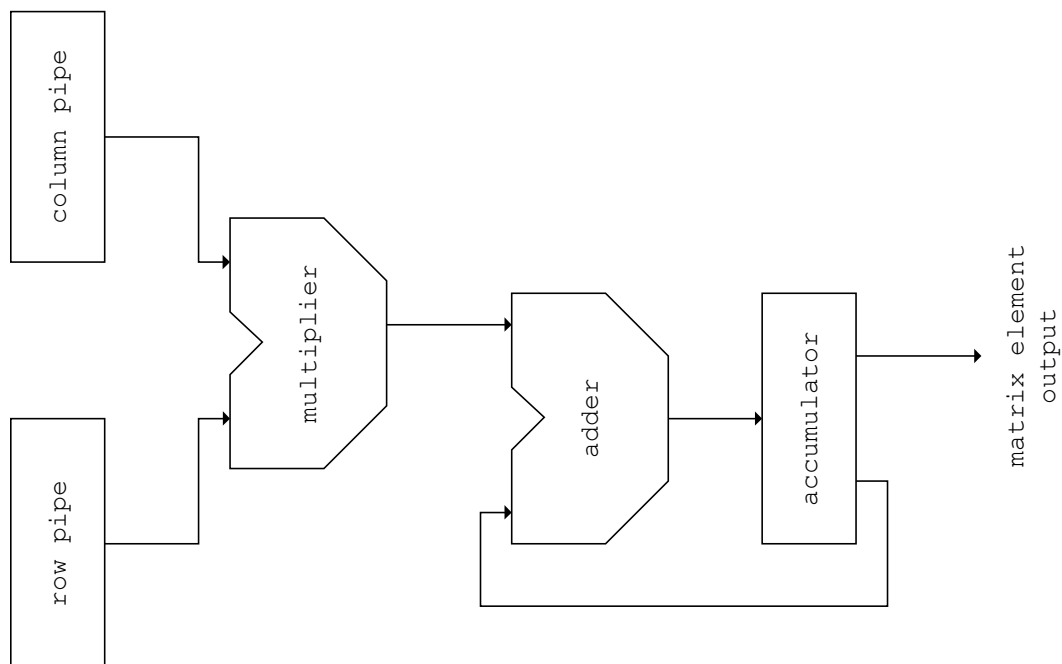


Figure 13: matrix multiplication basic module

The Element shown is capable of single matrix element calculation.

The matrix representation in a FPGA logic is also very problematic. Large matrices stored in the internal logic of FPGA take a huge amount of space. Using internal memory reduces it, unfortunately it doesn't allow to gain access to more than one matrix element at the same time. The representation should be chosen according to particular needs for user application.

### 3.4 IQ estimator

Output data of ADC can be interpreted as real part ( $x_k$ ) of analytic signal  $u(t) = u(kT) = u_k$  with unknown imaginary part ( $y_k$ ) for series of samples ( $k$ ).

$$u(k) = v(kT) \exp(i 2\pi f kT) = x_k + i y_k \quad \dots\dots$$

where  $v_k$  is decoded complex envelope of signal (with I and Q part)

Presented algorithm linearizes changes of envelope and eliminates offsets during period of carrier wave (4 us). Estimation schematic for 4 steps is shown in table. Each row in the table defines  $I_k$  and  $Q_k$  parts for given algorithm phase. In each phase 3 parts of the same part are estimated for following times:  $k-1$ ,  $k$ ,  $k+1$

for  $k-1$  – linear interpolation using  $x_k$  and  $x_{k-2}$

for  $k$  – calculation for current sample  $x_k$  with offset elimination

for  $k+1$  – prediction using  $x_k$  and  $x_{k-1}$

phase	Est. for $k-1$	Est. For $k$	Pred. For $k+1$	Est. For $k$
0	$I_{k-1} = (x_k - x_{k-2})/2$	$I_k = (x_k - \text{offset})$	$I_{k+1} = 2I_k - I_{k-1}$	$Q_k = 2Q_{k-1} - Q_{k-2}$
1	$Q_{k-1} = -(x_k - x_{k-2})/2$	$Q_k = -(x_k - \text{offset})$	$Q_{k+1} = 2Q_k - Q_{k-1}$	$I_k = 2I_{k-1} - I_{k-2}$
2	$I_{k-1} = -(x_k - x_{k-2})/2$	$I_k = -(x_k - \text{offset})$	$I_{k+1} = 2I_k - I_{k-1}$	$Q_k = 2Q_{k-1} - Q_{k-2}$
3	$Q_{k-1} = (x_k - x_{k-2})/2$	$Q_k = (x_k - \text{offset})$	$Q_{k+1} = 2Q_k - Q_{k-1}$	$I_k = 2I_{k-1} - I_{k-2}$

Table 5: IQ demodulation steps

Offset error for each phase is calculated using 3 samples:

$$\text{offset}_k = (x_{k-4} + 2x_{k-2} + x_k)/4$$

The result of the algorithm is I and Q part of an input signal which can be used in user algorithms.

### 3.5 CORDIC stage

The CORDIC [11] module executes a single iteration of the CORDIC algorithm, which is used to calculate magnitude and phase of a complex number. It also can be used to calculate values of cosine and sine functions. A single iteration is able to rotate a complex vector by a fixed angle using small amount of resources. It is done by multiplying a given vector by a fixed vector. The input vector is rotated left or right according to the sign of its imaginary part. Then the rotation angle is either added or subtracted from cumulative angle. Both the new vector and the updated cumulative angle are returned from the stage. The algorithm of single stage is shown on Figure 14.

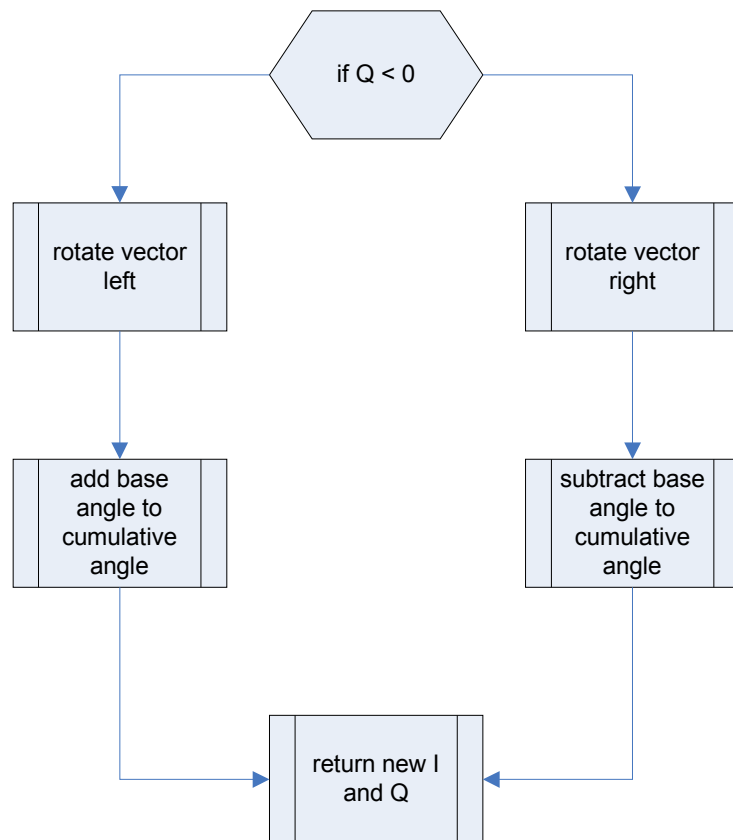


Figure 14: Algorithm executed by single CORDIC iteration

A single CORDIC stage uses no hardware multipliers, all rotations are done using only adders and shifters. Each stage adds the magnitude error to final result. This

error is called CORDIC GAIN. The size of this error depends on the rotation angle used by the stage and can be compensated after the last iteration.

### 3.6 Magnitude and Phase detector

Magnitude and phase calculation requires calculation of square root and arctan function. These functions are numerically complicated. FPGA chips have no hardware support for such operations. Fortunately both values can be calculated using multiple iterations of CORDIC algorithm. Each iteration of the algorithm performs rotation of a given vector towards zero. The rotation angle is cumulated, therefore the final phase result is the cumulated angle output from last iteration of the algorithm. The magnitude of an input vector equals the real part of an output vector from the last iteration of the algorithm ( after CORDIC GAIN compensation ). The angles of rotation and CORDIC GAIN for given iteration are shown in Table 6.

L	$K = 2^{-L}$	$B = 1 + jK$	angle	Magnit ude	CORDIC GAIN
0	1.0	$1 + j 1.0$	45.0000	1.4142	1.4142
1	0.5	$1 + j 0.5$	26.5650	1.1180	1.5811
2	0.25	$1 + j 0.25$	14.0362	1.0307	1.6298
3	0.125	$1 + j 0.125$	7.1250	1.0077	1.6424
4	0.0625	$1 + j 0.0625$	3.5763	1.0019	1.6456
5	0.03125	$1 + j 0.031250$	1.7899	1.0004	1.6464
6	0.015625	$1 + j 0.015625$	0.8951	1.0001	1.6466
7	0.007813	$1 + j 0.007813$	0.4476	1.0000	1.6467
	...	...	...	...	...

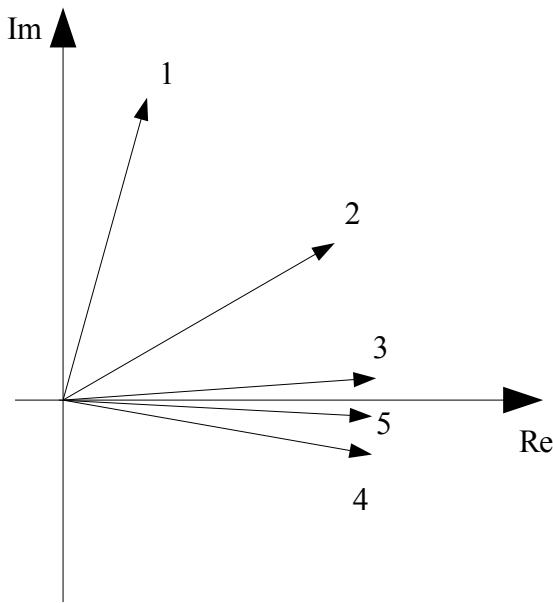
Table 6: CORDIC parameters for iterations

To calculate the magnitude and the phase of a complex number, the following steps must be executed:

- a) The sign of the imaginary part of the vector is checked and a rotation by +/-90 degrees is made. It moves the vector to the I or IV quarter of complex plane. The first rotation allows to calculate the vector's phase in a range from -180 to 180

degrees.

- b) Additional vector rotations are made by the angles show in Table 6. The direction of the rotation depends on the sign of the imaginary part of current vector
- c) After N iterations the imaginary part of a vector is close to 0. After CORDIC GAIN correction, the real part of the vector is the magnitude and phase of the vector equals cumulated angle form last iteration.



- 1. Vector is rotated by 45 degrees towards 0. Cumulative angle is set to 45
- 2. Next rotation by ~26 degrees is made. Cumulative angle is set to 71
- 3. Next rotation by ~14 sets cumulative angle to 85
- 4. Rotation by -7 is done ( towards 0) Cumulative angle equals 78
- 5. Final vector. Phase error after 4 iterations was ~4 degrees.

Figure 15: Procedure of magnitude and phase calculation using CORDIC

### 3.7 Sin/Cos calculation

The problem of calculating sin and cos values for a given angle  $\varphi$ , can be reduced to search of a complex number with magnitude of 1 and phase  $\varphi$ .

$$|A| \exp(j\varphi) = |A| ( \cos(\varphi) + j \sin(\varphi) )$$

Then the real part of such number equals cos of the angle and imaginary part equals sin of the angle. The procedure of the calculation for both functions is shown on Figure 16.

1. The starting point for the algorithm is A:

$$A = \begin{cases} j & \varphi > 90^\circ \\ -j & \varphi < -90^\circ \\ 1 & \text{when others} \end{cases}$$

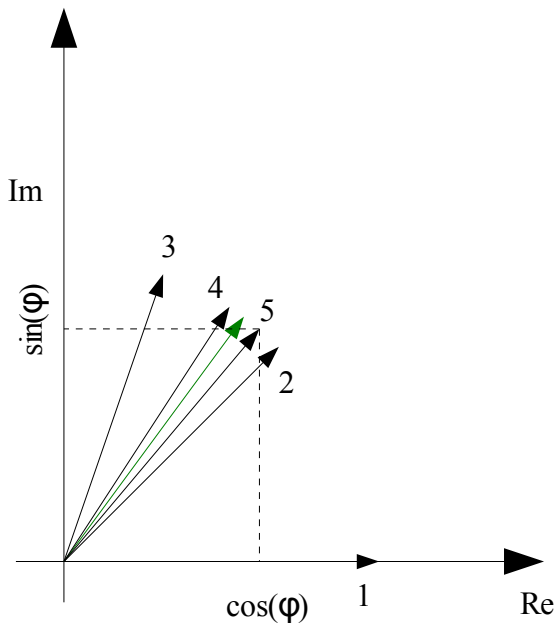
2. In the next steps, rotations of the vector are made according to Table. The rotation is executed towards the angle  $\varphi$ . After N iterations the vector A' close to the searched vector is calculated:

$$A' = I_a' + jQ_a' = |A'| ( \cos(\varphi) + j\sin(\varphi) )$$

After CORDIC GAIN compensation:

$$\cos(\varphi) = I_a'$$

$$\sin(\varphi) = Q_a'$$



1. Vector is rotated by 45 degrees towards target vector ( green ) Cumulative angle is set to 45

2. Next rotation by ~26 degrees is made. Cumulative angle is set to 71

3. Next rotation by -14 sets cumulative angle to 57

4. Rotation by -7 is done ( towards green vector) Cumulative angle equals 50

5. Final vector. Phase error after 4 iterations was ~3 degrees

Figure 16: Procedure of sin/cos calculation

### 3.8 SRT stage

The SRT [12] algorithm is an iterative algorithm used for integer division. It was discovered at about the same time by Sweeney, Robertson and Tocher (SRT). It is used in many popular microprocessors such as Intel Pentium. This module executes the single iteration of the SRT algorithm. The algorithm can be described by the following equation:

$$r_i = \beta r_{i-1} - q_i D$$

where

$r_i$  – partial remainder calculated in this iteration

$r_{i-1}$  - partial remainder from previous iteration

$\beta$  – radix (  $2^m$  )

$D$  – divisor

$q_i$  – quotient digit for this iteration

The choice of the radix determines the complexity of the whole algorithm. A higher radix reduces the latency but increases the quotient digit set which leads to a high logical complexity of a single stage ( therefore reduces maximum frequency ). For higher radix division it is possible to use look up tables instead of logical comparators, but the size of this table increases exponentially.

The quotient digit set for a radix 2 SRT algorithm is fairly simple:

$$\{ -1, 0, 1 \}$$

Therefore the logic required for a single stage is simple and works with high frequency. Unfortunately the latency is also very high – number of clock cycles required to get the result equals to the bit width of the dividend. The general rule for quotient digit selection for single stage is:

$$q_i = \begin{cases} 1 & \text{if } 2r_{i-1} \geq 1/2 \\ 0 & \text{if } -1/2 \leq 2r_{i-1} < 1/2 \\ \bar{1} & \text{if } 2r_{i-1} < -1/2. \end{cases}$$

The decision can be made using only two most significant bits of partial remainder.

One of possible quotient digit sets for radix 4 SRT algorithm is:

$$\{-2, -1, 0, 1, 2\}$$

Logic required for quotient digit selection is complicated, but in this case look up table has reasonable size. The latency introduced by this approach is two times smaller than for radix 2.

The measure of redundancy for this set can be calculated using formula:

$$k \leq \alpha/(\beta-1)$$

Where  $\beta$  is radix of algorithm and  $\alpha$  is absolute maximum value from digit set. In this case  $k = 2/3$ . The values of  $k$  closer to 1 mean greater redundancy in digit set. Regions for digit selection can be described as:

$$-2/3 + q \leq 4r_{i-1}/D \leq 2/3 + q$$

This regions are shown on Figure 17

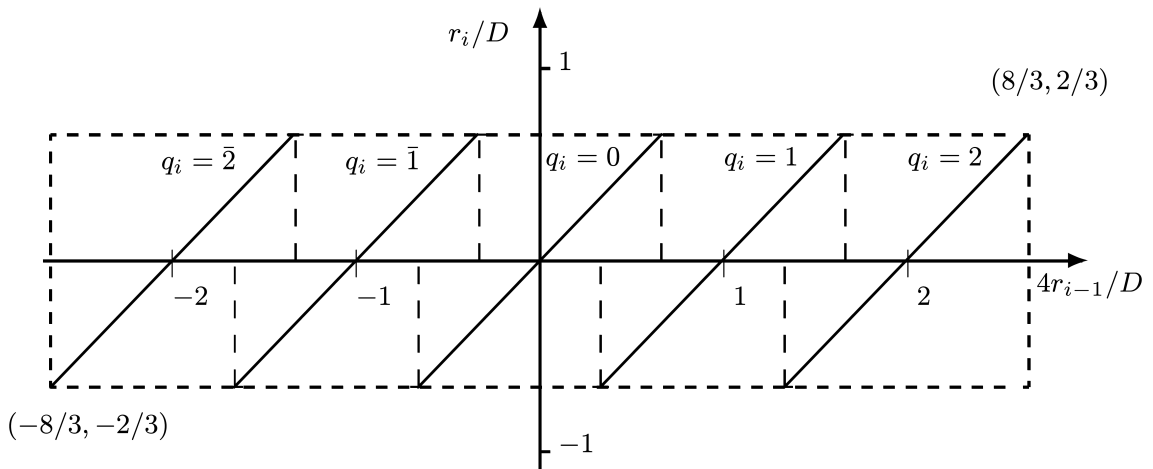


Figure 17: Quotient selection regions for SRT algorithm

As one can see regions are overlapping. This is caused by the redundancy in digit set. Higher redundancy means more overlapping and a logic reduction for digit selection.

Partial remainder vs. divisor plot is shown on Figure 18. This plot shows overlapped quotient digit selection regions together with decision lines for each digit.

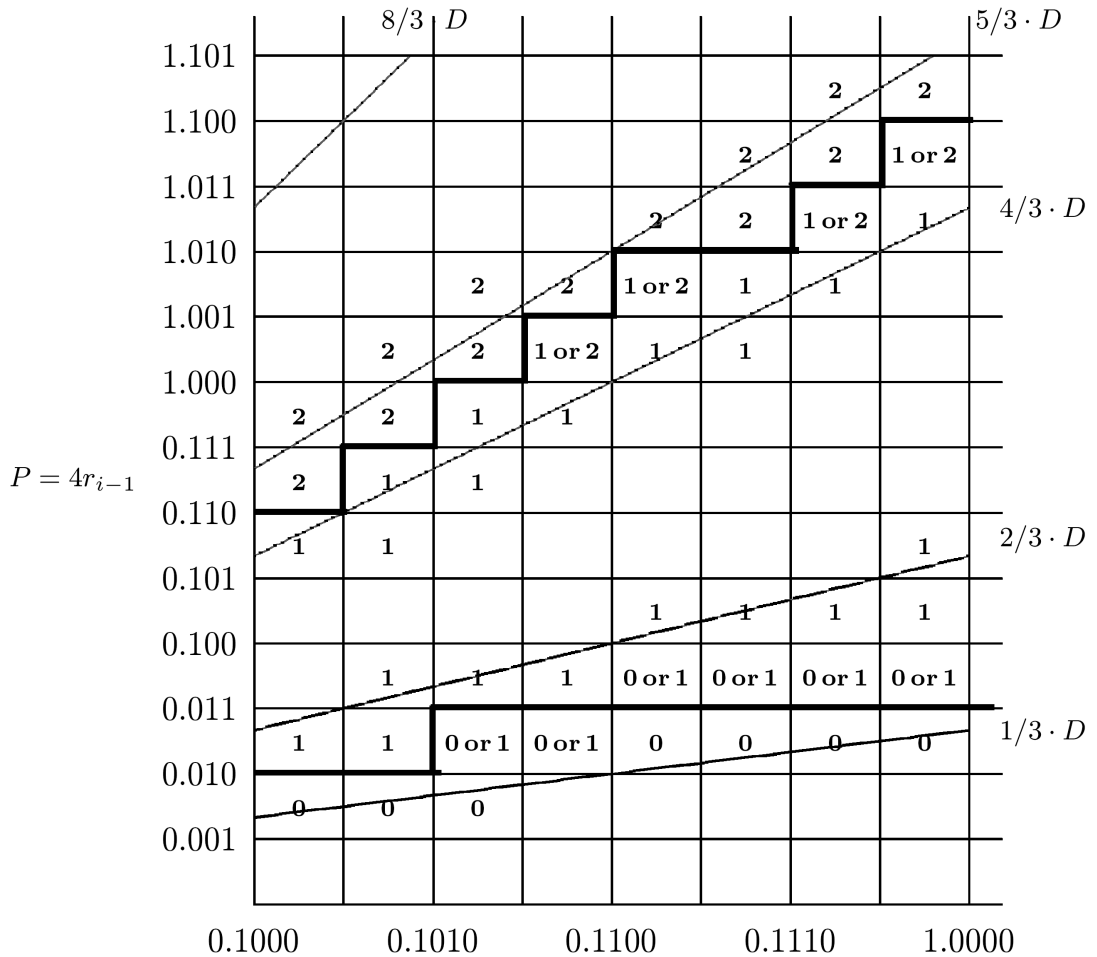


Figure 18: Partial remainder vs. divisor plot for SRT radix 4 algorithm

It can be used for look up table generation. The index for the table are most significant digits of the partial remainder and divisor. The values in the table are digits for each region.

### 3.9 Fixed point divider

Using modules the described in the previous chapter, a fixed point divider was created. The modules are cascaded. The theoretical latency of the divider equals N clock cycles for N bit integers ( using SRT radix 2 module ) and N/2 clock cycles ( using SRT radix 4 module)

### 3.10 Floating point unit

A floating-point number  $a$  can be represented by two numbers  $m$  and  $e$ , such that  $a = m \times b^e$ . In any such system a base  $b$  is picked (called the base of numeration, also the radix) and a precision  $p$  (how many digits to store).  $m$  (which is called the significand or, informally, mantissa) is a  $p$  digit number of the form  $\pm d.ddd\dots ddd$  (each digit being an integer between 0 and  $b-1$  inclusive). If the leading digit of  $m$  is non-zero then the number is said to be normalized. Some descriptions use a separate sign bit ( $s$ , which represents  $-1$  or  $+1$ ) and require  $m$  to be positive.  $e$  is called the exponent. This scheme allows a large range of magnitudes to be represented within a given size of field, which is not possible in a fixed-point notation. The floating-point representation is regulated by the IEEE 754 [20] standard.

This unit can perform basic arithmetical operation on a single precision floating point number ( 32 bits – 1 bit sign, 23 bit significand and 8 bit exponent ).

The basic structure of multiplication and division is

1. significands of both numbers are multiplied/divided and exponents are added/subtracted
2. normalization of result is made
3. rounding of final result is made and result's sign is calculated

The structure of an adder/subtractor is more complicated:

1. Numbers are denormalized to have the same exponents
2. significands are added/subtracted, an exponent decision is made
3. the result is normalized
4. rounding of final result is made and result's sign is calculated

IEEE754 defines four rounding schemes. In this library only one was implemented. All arithmetic operation use 'round towards zero' scheme.

### **3.11 OPB wrapper**

The 'Onboard Peripheral Bus' is one of communication busses for embedded PowerPC used by Xilinx company. Each device connected to this bus can be mapped into embedded system's address space and then referenced from software. This wrapper provides an easy to use interface between the described components ( or any user component ) and OPB bus. This approach provides a completely new procedure for the algorithm development. At first, algorithms can be implemented using a programming language such as C or C++. Then, when the functionality is checked, all time critical parts can be easily moved into the hardware. This speeds up algorithm development and tests.

### **3.12 Summary**

Some of the described library blocks (such as division, matrix operations) solve problems which were hard to overcome during the implementation process. Operations like division are difficult to implement. Other components allow users to simplify their implementation and reduce implementation time. Moreover each of the modules can become basis for further library development. User can design his own problem specific

components and include them in extension library. Modular library provides easy way for possible updates. It is only necessary to change component inside library. Changes will be visible in every implementation.

Moreover all used algorithms and concepts are well known in DSP processing. They were tested in a long period of time. A good example is the IQ demodulation algorithm which is currently used in the FPGA controller for the ACC1 module and the RF\_GUN at the VUV-FEL. The SRT algorithm is commonly used as a division algorithm in many modern microprocessors such as Intel Pentium. The concept of saturated arithmetics is also well known and implemented in many programming languages.

Chapter 4 describes implementation of each module – its interface and basic functionality. Described modules were grouped into libraries and implemented to meet performance goals set by target environment.

## 4. Implementation

Described modules were implemented using the VHDL description language. The code is prepared to be synthesized using most common compilers. It is VHDL'93 standard compliant.

The code is based on three packages from the IEEE library:

- `std_logic_1164`
- `std_logic_signed`
- `std_logic_unsigned`

This packages provide a basic interface for arithmetical operations and type conversions. In some modules it was necessary to use `std_logic_arith` for some additional functions for variable conversions. In this chapter the implementation of each of the modules will be described

### 4.1 `math_basic_unsigned`

This module provides a basic interface for unsigned arithmetical operations for other modules. It consists of following functions:

```
Vcreate(arg : natural ; length : integer ) return std_logic_vector
```

Function *Vcreate* is a wrapper for `CONV_STD_LOGIC_VECTOR` function from IEEE library. It converts integer value to its binary representation.

```
Vresize (arg : std_logic_vector ; length : natural ) return  
std_logic_vector
```

Function *Vresize* is a function for vector resizing. It is basic function for

saturation control in the whole library. The algorithm executed by this function is shown on Figure 19.

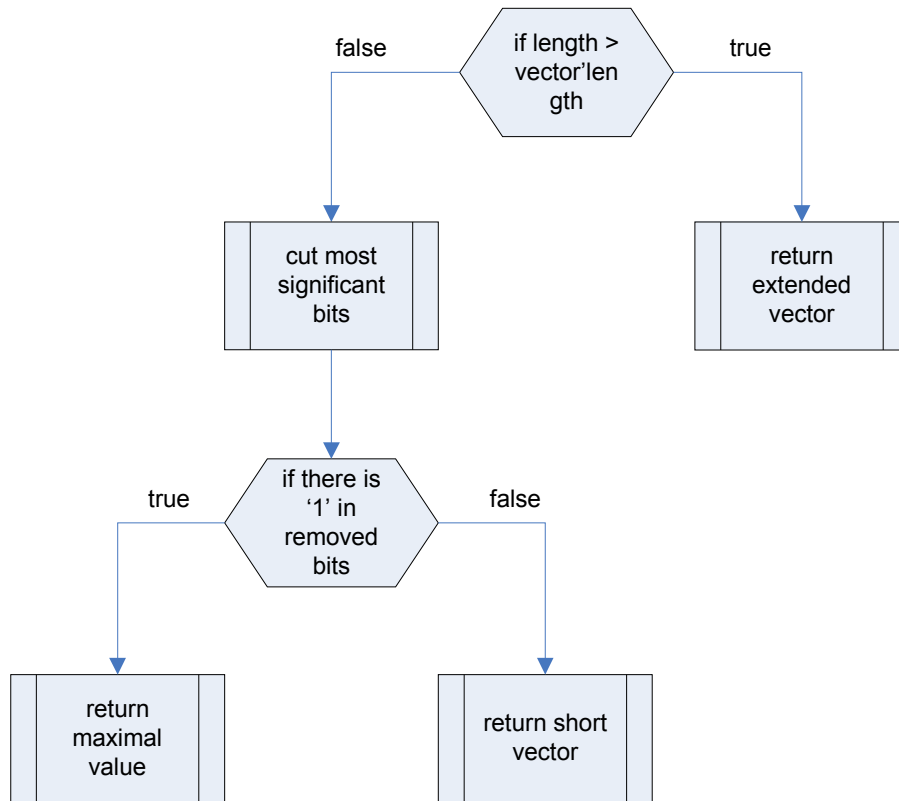


Figure 19: Saturation control algorithm

```

VShiftLeft(arg : std_logic_vector ; shift : natural ) return
std_logic_vector
VShiftRight(arg : std_logic_vector ; shift : natural ) return
std_logic_vector
VShift      (arg : std_logic_vector ; shift : integer ) return
std_logic_vector
  
```

The function *Vshift* uses *VshiftRight* and *VshiftLeft* functions to shift it's argument by N bits left or right ( when -N given as shift ). Shift must be a static expression – fixed shifters are synthesized during compilation process.

```

VSum (arg1,arg2 : std_logic_vector ; length : natural ) return
std_logic_vector
VSub (arg1,arg2 : std_logic_vector ; length : natural ) return
std_logic_vector
VMult(arg1,arg2 : std_logic_vector ; length : natural ) return
std_logic_vector
  
```

*Vsum*, *Vsub* and *Vmult* functions are wrappers for operators '+', '-' and '\*' defined in `std_logic_unsigned` package with additional saturation control. Algorithms executed by these functions are shown on Figure 20.

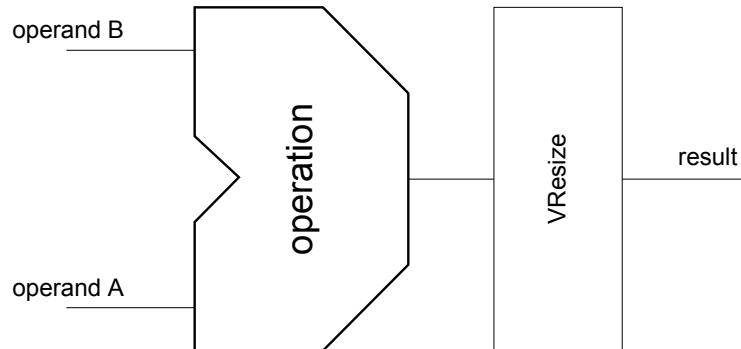


Figure 20: Structure of arithmetic operations

## 4.2 math\_basic\_signed

The module provides a basic interface for signed arithmetical operations for other modules. The following functions are defined:

```

SVCreate(arg : integer ; length : integer) return SV ;
SVResize(arg : SV ; length : natural ) return SV;

SVShiftLeft (arg : SV ; shift : natural ) return SV ;
SVShiftRight (arg : SV ; shift : natural ) return SV ;
SVShift (arg : SV ; shift : integer ) return SV ;

SVSum (arg1,arg2 : SV ; length : natural ) return SV ;
SVSub (arg1,arg2 : SV ; length : natural ) return SV ;
SVMult(arg1,arg2 : SV ; length : natural ) return SV ;
  
```

where SV is an alias for a `std_logic_vector`.

The main difference between modules is that signed module is based on `ieee.std_logic_signed` while unsigned is based on `ieee.std_logic_unsigned`. Functions redefined for this library perform the same function as similar functions in unsigned library. The major difference is in *SVResize* function. It is base for saturation control for signed arguments. The algorithm executed by this function is shown on Figure 21.

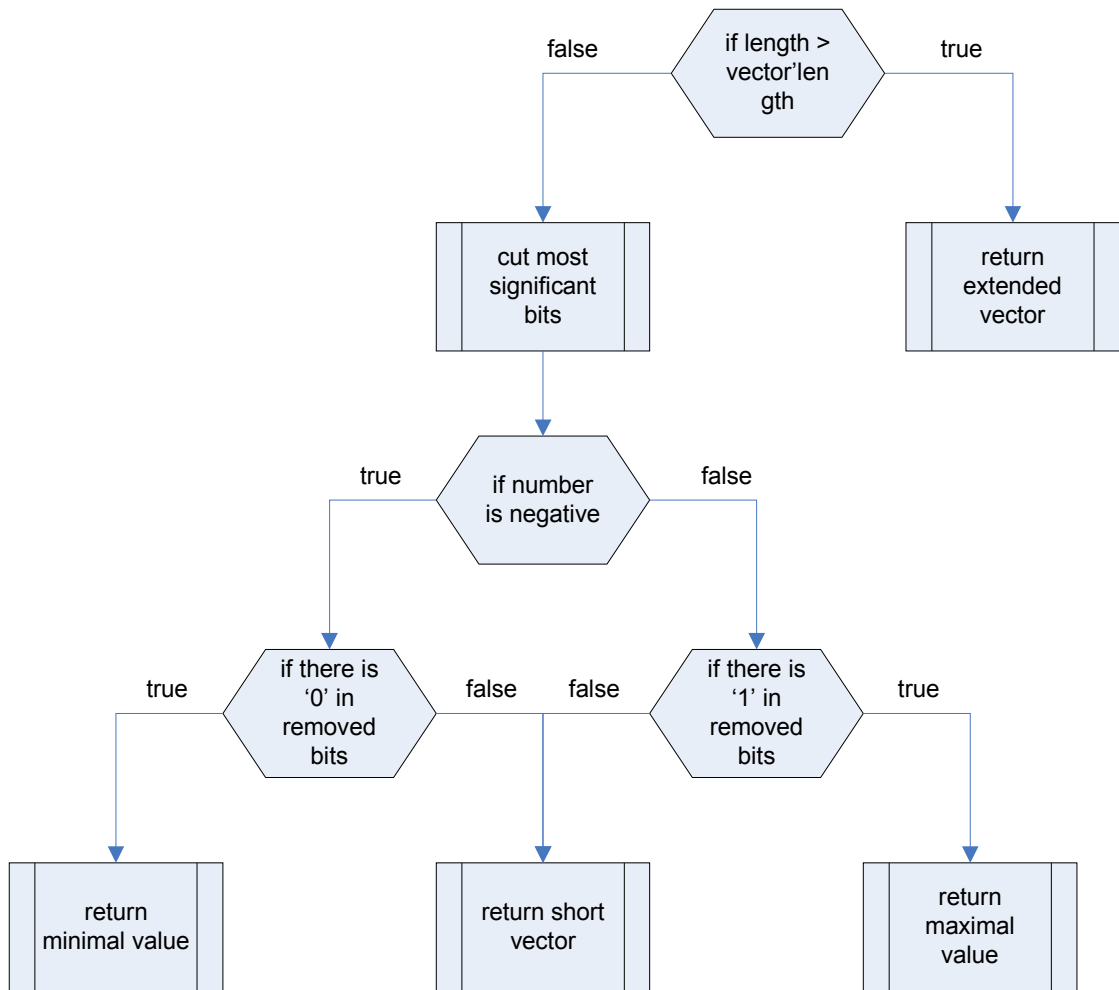


Figure 21: Saturation control for signed vectors

Two additional functions:

```
SVNeg(arg : SV ) return SV ;
SVAbs(arg : SV ) return SV ;
```

are directly connected to signed representation

*SVNeg* function executes following code:

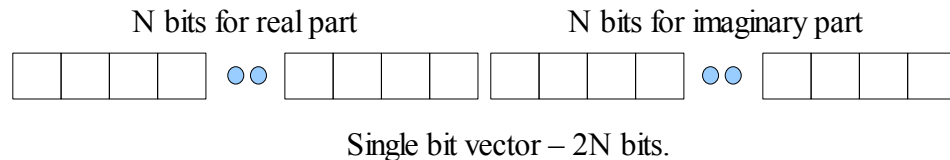
```
result := not arg ;
return result+1 ;
```

This formula is directly taken from two's complement definition.

The function *SVAbs* executes the function *SVNeg* conditionally ( when the sign of an argument is '-').

### 4.3 math\_complex

This module provides complex number signed arithmetic operators. The representation of complex number was chosen to simplify operations. It is shown below:



The following functions are defined in this module:

```
SCCreate( re,im : TSV) return TSC ;  
SCCreate( re,im,length : integer ) return TSC ;
```

The functions *SCCreate* create complex number in representation shown using two signed vectors or two integers using length bits.

```
SCResize( arg : TSC ; length : integer ) return TSC ;
```

The function *SCResize* provides tool for both imaginary and real part resizing using saturation control presented earlier.

```
SCReal( arg : TSC ) return TSV ;  
SCImag( arg : TSC ) return TSV ;
```

Functions *SCReal* and *SCImag* return real and imaginary part from vector representation of a complex number

```
SCSum( arg1,arg2 : TSC ; length : natural ) return TSC ;  
SCSub( arg1,arg2 : TSC ; length : natural ) return TSC ;  
SCMult( arg1,arg2 : TSC ; length : natural ) return TSC ;
```

The arithmetical operations are executed according to the algorithms presented on Figure 22 and Figure 23.

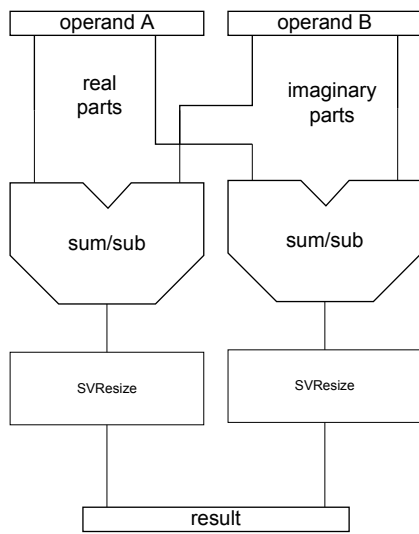


Figure 22: Complex add/sub

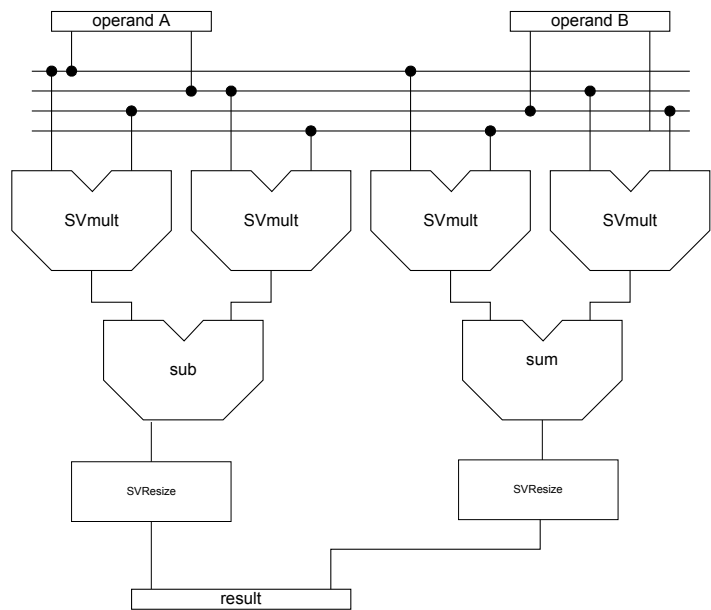


Figure 23: Complex multiplication

```
SCNeg( arg : TSC ) return TSC ;
```

The Function *SCNeg* inverts the sign of both real and imaginary part of complex vector. It rotates the signal by 180 degrees.

## 4.4 math\_matrix

This library defines basic components for matrix operations such as multiplication and addition.

The main component for a matrix multiplication is a multiplier with accumulator. The interface to the component is shown below.

```
component matrix_mult_base is
  generic (
    INPUT_WIDTH      : natural := 18 ;
    INTERNAL_WIDTH    : natural := 32 ;
    OUTPUT_WIDTH      : natural := 18 ;
    BASE               : natural := 0
  ) ;
  port (
    resetN           : in  std_logic ;
    clk               : in  std_logic ;
```

```

        r_in  : in  std_logic_vector( INPUT_WIDTH-1 downto 0) ;
        c_in  : in  std_logic_vector( INPUT_WIDTH-1 downto 0) ;

        i_out : out std_logic_vector(OUTPUT_WIDTH-1 downto 0)
    ) ;
end component ;

```

Parameters:	
INPUT_WIDTH	defines width of single matrix element
INTERNAL_WIDTH	defines width of internal accumulator
OUTPUT_WIDTH	defines width of output result
ITEM_COUNT	Number of items in single matrix row/column
BASE	defines number of fractional bits in output data.

Ports:	
resetN	port used to reset internal registers such as accumulator
clk	clocking port
r_in	vectors connected to pipes/memories with row elements
c_in	vectors connected to pipes/memories with column elements
i_out	output element of result matrix

This component can be used to calculate a single element of the matrix C where  
 $C = A*B$

both A and B are matrices of sizes which allow multiplication

When the data pipe provides more than one row/column of matrix, this component can calculate several elements of matrix C. Latency of the component equals size of matrix row in clock cycles and for more than one element calculation it is multiplied by number of elements.

The second component defined in this library is component which allows to calculate one or more elements of matrix C where:

$$C = A+B \text{ or } C = A-B$$

The interface of the component is:

```

component matrix_sum_base is
    generic (
        INPUT_WIDTH      : natural := 18 ;
        OUTPUT_WIDTH     : natural := 18
    ) ;
    port (
        resetN           : in  std_logic ;
        clk              : in  std_logic ;

        rA_in : in  std_logic_vector( INPUT_WIDTH-1 downto 0) ;
        rB_in : in  std_logic_vector( INPUT_WIDTH-1 downto 0) ;

        r_out : out std_logic_vector( OUTPUT_WIDTH-1 downto 0)
    ) ;
    op      : in std_logic
end component ;

```

Parameters:	
INPUT_WIDTH	defines width of a single matrix element
OUTPUT_WIDTH	defines width of the output result

Ports:	
resetN	port used to reset internal registers such as accumulator
clk	clocking port
rA_in	vectors connected to pipes/memories with A row elements
rB_in	vectors connected to pipes/memories with B row elements
r_out	output element of result matrix
op	Defines operation: '0' – A+B, '1' – A-B

## 4.5 IQ demodulator

This library defines the module for IQ demodulation. The interface of the component is shown below:

```

component IQdet is
    generic (
        DSP_WIDTH : natural := 18
    ) ;
    port (
        resetN      : in  std_logic ;
        lclk        : in  std_logic ;
        adc_sample  : in  TSV(DSP_WIDTH-1 downto 0) ;
        I           : out TSV(DSP_WIDTH-1 downto 0) ;
        Q           : out TSV(DSP_WIDTH-1 downto 0)
    ) ;
end component ;

```

Parameters:	
DSP_WIDTH	defines width of input elements

Ports:	
resetN	port used to reset internal registers such as accumulator
lclk	clocking port
adc_sample	Raw signal for I and Q calculation
I,Q	I and Q outputs

This component is capable of IQ demodulation. It was implemented according to the mathematical formulas described in chapter 3.4.

## 4.6 CORDIC

This library defines modules for cordic algorithm. Two functions defined in this module are:

```

function complex_rotate_I( tI,tQ : TSV ; N : TN ) return TSV ;
function complex_rotate_Q( tI,tQ : TSV ; N : TN ) return TSV ;

```

They are used to calculate coordinate of vector after rotation. Rotations are made according to CORDIC definition for N<sup>th</sup> iteration. The following component is able to perform a single step of the CORDIC algorithm. Its interface is shown below.

```

component cordic is
generic (
    IQ_WIDTH      :    natural    := 18 ;
    IQ_LEVEL      :    natural    := 0
) ;
port (
    clk           : in std_logic ;
    resetN       : in std_logic ;

    I            : in TSV(IQ_WIDTH-1 downto 0) ;
    Q            : in TSV(IQ_WIDTH-1 downto 0) ;

    newI         : out TSV(IQ_WIDTH-1 downto 0) ;
    newQ         : out TSV(IQ_WIDTH-1 downto 0) ;

    phase_in     : in  TSV(IQ_WIDTH-1 downto 0) ;
    phase_out    : out TSV(IQ_WIDTH-1 downto 0) ;

    BASE_ANGLE   : in  TSV( IQ_WIDTH-1 downto 0 )
) ;
end component ;

```

Parameters:	
IQ_WIDTH	defines width of input elements
IQ_LEVEL	defines iteration number executed by this component ( rotation functions depend on this parameter )

Ports:	
resetN	port used to reset internal registers such as accumulator
clk	clocking port
I,Q	I and Q input vector coordinates
newI,newQ	coordinates of rotated vector

Ports:	
BASE_ANGLE	value of rotation angle executed by this stage
phase_in	cumulativ phase input
phase_out	cumulative phase output ( phase_in + BASE_ANGLE or phase_in - BASE_ANGLE )

In this approach a BASE\_ANGLE can be changed during operation which allows extended algorithm control. When it is not necessary BASE\_ANGLE can be moved to parameters list to reduce resources consumption. The general rule of operation is described in chapter 3.5

Second component defined in this library is component for amplitude and phase calculation. Its interface is:

```

component cordicAP is
generic (
    IQ_WIDTH          :    natural    := 18 ;
    CORDIC_LEVELS    :    natural    := 0
) ;
port (
    clk                : in std_logic ;
    resetN             : in std_logic ;

    I                  : in TSV(IQ_WIDTH-1 downto 0) ;
    Q                  : in TSV(IQ_WIDTH-1 downto 0) ;

    magnitude         : out TSV(IQ_WIDTH-1 downto 0) ;
    phase              : out TSV(IQ_WIDTH-1 downto 0)
) ;
end component ;

```

Parameters:	
IQ_WIDTH	defines width of input elements
CORDIC_LEVELS	defines number of iterations executed by component

Ports:	
resetN	port used to reset internal registers such as accumulator
clk	clocking port
I,Q	I and Q input vector coordinates

Ports:	
magnitude	magnitude result of input vector
phase	phase result for IQ vector

This component creates multiple instances of CORDIC stage entity to execute several iterations of CORDIC algorithm. The description can be found in chapter 3.6

## 4.7 SRT

This library consists of the following components with the same interface, which execute a single iteration of the SRT algorithm

First component executes single step of radix-2 srt algorithm:

```

component srt_stage2 is
  generic (
    WORD_WIDTH : natural := 18
  ) ;
  port (
    clk          : in  std_logic ;
    resetN       : in  std_logic ;

    Pin          : in  TSV(WORD_WIDTH-1 downto 0) ;
    Pout         : out TSV(WORD_WIDTH-1 downto 0) ;

    D            : in  std_logic_vector(WORD_WIDTH-1 downto 0) ;
    Dout         : out std_logic_vector(WORD_WIDTH-1 downto 0) ;

    i_result     : in  TSV(WORD_WIDTH-1 downto 0) ;
    o_result     : out TSV(WORD_WIDTH-1 downto 0)
  ) ;
end component;

```

The second one executes single step of radix-4 srt algorithm

```

component srt_stage4 is
  generic (
    WORD_WIDTH : natural := 18
  ) ;

```

```

port (
    clk          : in  std_logic ;
    resetN       : in  std_logic ;

    Pin          : in  TSV(WORD_WIDTH-1 downto 0) ;
    Pout         : out TSV(WORD_WIDTH-1 downto 0) ;

    D            : in  std_logic_vector(WORD_WIDTH-1 downto 0) ;
    Dout         : out std_logic_vector(WORD_WIDTH-1 downto 0) ;

    i_result     : in  TSV(WORD_WIDTH-1 downto 0) ;
    o_result     : out TSV(WORD_WIDTH-1 downto 0) ;
);
end component;

```

Parameters:	
WORD_WIDTH	defines width of input elements

Ports:	
resetN	port used to reset internal registers such as accumulator
clk	clocking port
Pin,Pout	input partial remainder and output partial remainder after iteration
Din,Dout	pipeline for divisor
i_result	result calculated in previous iteration
o_result	result updated in this iteration

The component is described in chapter 3.8. These components were used to create a fixed point divisor which can execute a fixed point division of numbers normalized to the  $[0.5,1)$  range. Multiple instances of the SRT stage were used. Each stage is capable of one ( SRT2 ) or 2 ( SRT4 ) digits of quotient calculation. It is defined as follows:

```

component srt2/srt4 is
    generic (
        WORD_WIDTH : natural := 18
    );
    port (
        clk          : in  std_logic ;
        resetN       : in  std_logic ;

```

```

D          : in  std_logic_vector(WORD_WIDTH-1 downto 0) ;
C          : in  std_logic_vector(WORD_WIDTH-1 downto 0) ;

W          : out std_logic_vector(WORD_WIDTH-1 downto 0) ;
R          : out TSV(WORD_WIDTH  downto 0)
);
end component;

```

Parameters:	
WORD_WIDTH	defines width of input elements and number of iterations needed to get full result

Ports:	
resetN	port used to reset internal registers
clk	clocking port
D	divisor input
C	dividend input
W	result
R	remainder

## 4.8 Floating point unit

The floating point unit consists of 3 components capable of arithmetic operations on floating point numbers ( compatible with IEEE 784 standard ). The interface of the components is shown below.

```

component mult[div/sum]_float is
  port (
    clk          : in  std_logic ;
    resetN       : in  std_logic ;

    S1           : in  std_logic ;
    S2           : in  std_logic ;

    E1           : in  std_logic_vector(7 downto 0) ;
    E2           : in  std_logic_vector(7 downto 0) ;

    M1           : in  std_logic_vector(22 downto 0) ;
    M2           : in  std_logic_vector(22 downto 0) ;
  );
end component;

```

```

        S3          : out std_logic ;
        E3          : out std_logic_vector( 7 downto 0) ;
        M3          : out std_logic_vector(22 downto 0)
    );
end component ;

```

Ports:	
resetN	port used to reset internal registers
clk	clocking port
S1,S2	signs of operands
S3	sign of the result
E1,E2	exponents of operands
E3	exponent of result
M1,M2	mantisas of operands
M3	mantisa of reult

The components are fully pipelined therefore processing of the operands can start before the result of the previous ones is ready. The structure of the components is shown on Figure 24 and Figure 25.

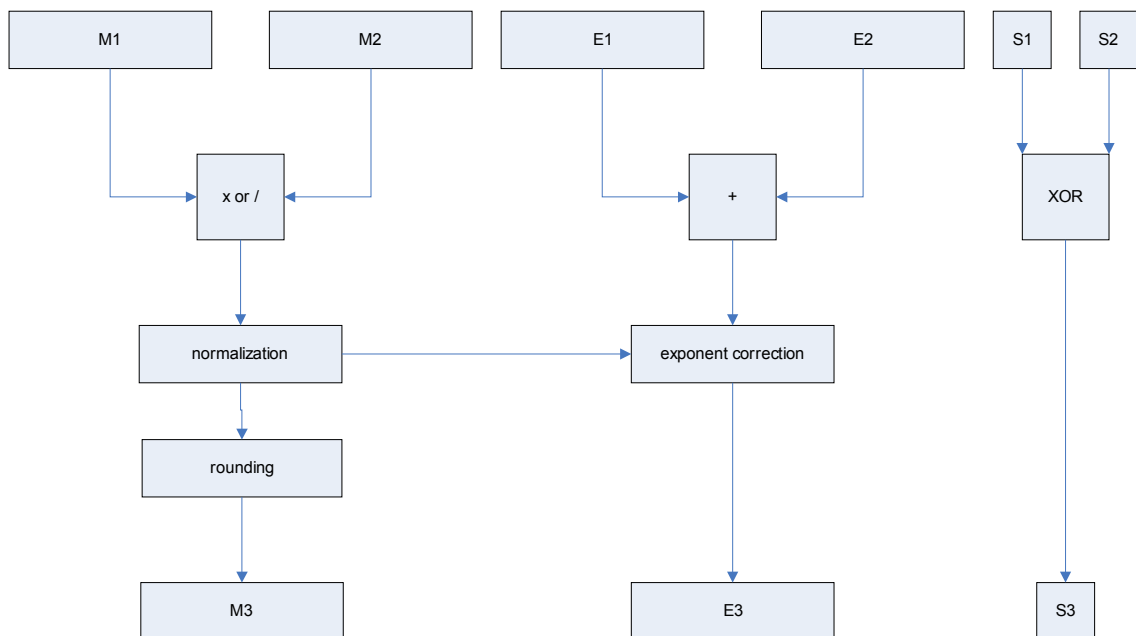


Figure 24: Floating point multiplication/division structure

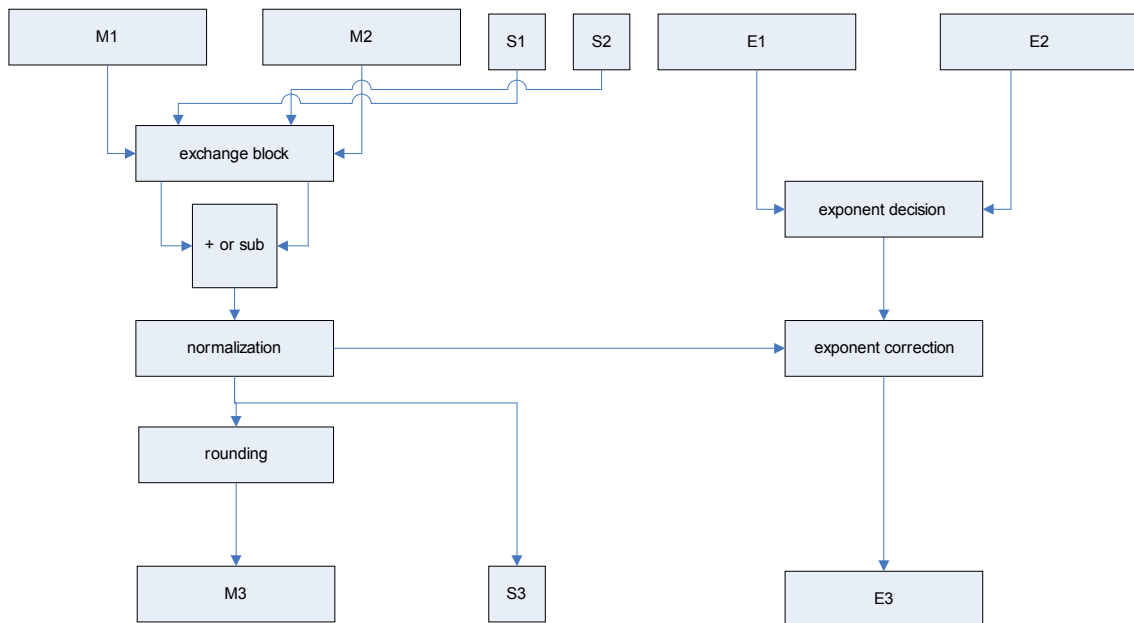


Figure 25: Floating point adder structure

A functional description of the floating point arithmetic operations can be found in chapter 3.10.

## 4.9 FIR filter

This FIR filter is a flexible, programmable filter. Modifications of filter parameters and filter order do not require program recompilation. The following declaration shows component's interface.

```
Type Tarray is array(31 downto 0) of natural ;
```

```
component filter is
```

```
  generic (
```

```
    WORD_WIDTH : natural := 18 ;
```

```
    MAX_ORDER  : natural := 32
```

```
  ) ;
```

```
  port(
```

```
    clk           :in  std_logic ;
```

```
    int_clk       :in  std_logic ;
```

```
    resetN        :in  std_logic ;
```

```
    order         :in  natural  ;
```

```
    coefficients  :in  Tarray
```

```

    in_data      : in   std_logic_vector(WORD_WIDTH-1 downto 0) ;
    out_data     : out  std_logic_vector(WORD_WIDTH-1 downto 0)
);
end component;

```

Parameters:	
WORD_WIDTH	defines width of input elements
MAX_ORDER	defines maximum order of the filter ( set at compialtion time)

Ports:	
resetN	port used to reset internal registers
clk	clocking port
int_clk	clocking port used for internal calculations
order	Actual order of the filter
coefficients	table of coeficients
data_in	data input for the filter
data_out	filtered data

The maximum value of 'order' port is MAX\_ORDER. When it exceeds this parameter it is treated as MAX\_ORDER. CLK and INT\_CLK can be connected to the same clock if the sampling speed needs to be exactly the same as processing speed.

The structure of the implemented filter is shown on Figure 26.

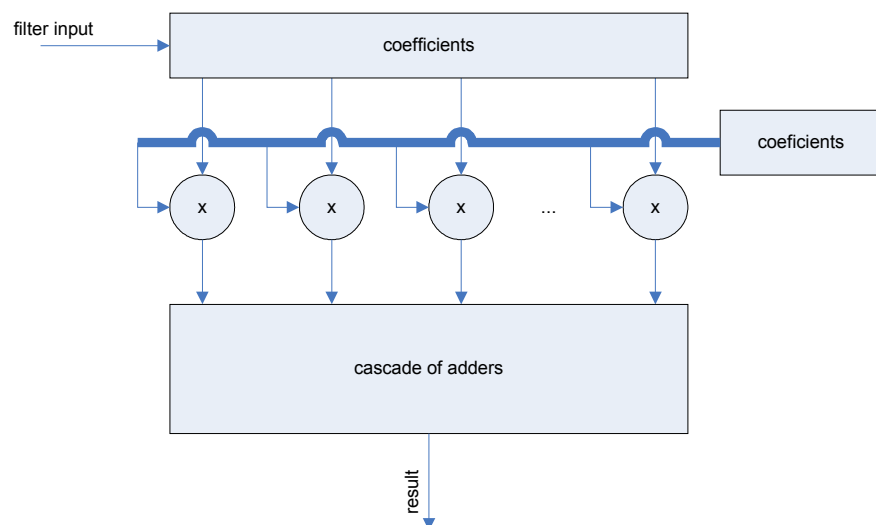


Figure 26: Structure of a programmable filter

## 4.10 OPB wrapper

This component is based on a OPB peripheral template provided by XILINX. It provides the OPB interface for components defined in the mathematical library or for any user component. Typical transactions on the OPB bus is shown on Figure 27.

Wrapper defines a set of registers which are mapped into embedded system's address space. Register can be connected to any signal in the VHDL code. The component is compatible with the Xilinx EDK IP core definition so it can be added to embedded system using a graphical tool. Internal structure of this wrapper is shown in Figure 27.

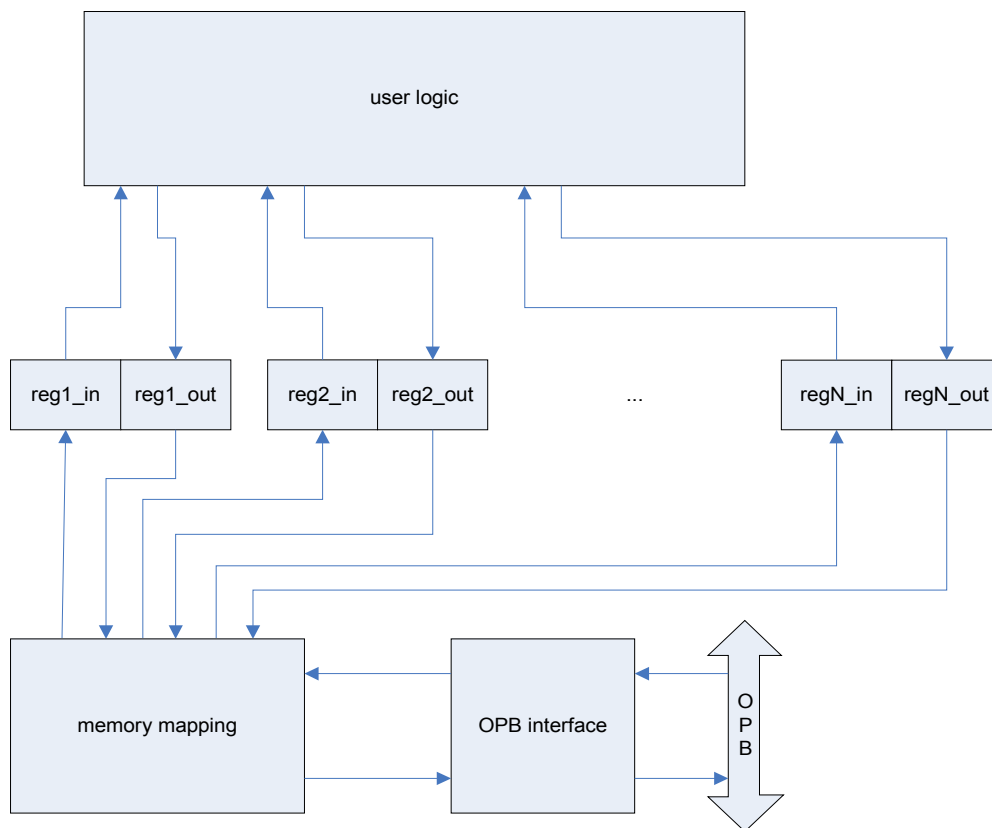


Figure 27: OPB wrapper structure connected to OPB logic

## 4.11 Summary

As the result of the implementation of the concept shown in chapter 3, a flexible mathematical library was created. It fulfills all the requirements for the system described in chapter 2. The functional blocks such as IQ demodulator or magnitude and phase calculation provide scalable and simple means to implement input stages of many algorithms. Blocks for matrix multiplication, division and sine calculation can be used in many different places inside the algorithm implementation ( for example inside detuning algorithm implementation or controller structures ). The rest of the basic blocks such as `math_basic_signed` or `math_matrix` modules can be used when functionality not included in this library is needed. They allow low level algorithm implementation.

All blocks were optimized to provide a resonable choice between performance and resource usage according to possibilities in the target accelerator environment. After and during implementation all modules were completely tested. Descriptions and the results of tests are shown in chapter 5.

## 5. Tests of designed system

All parts of presented system were tested during implementation using VHDL simulation environment ( Aldec ActiveHDL ). The test procedure is shown using the `matrix_mult_base` component as example. The first step was the implementation of the module. The layout of ActiveHDL design environment is shown on Figure 28.

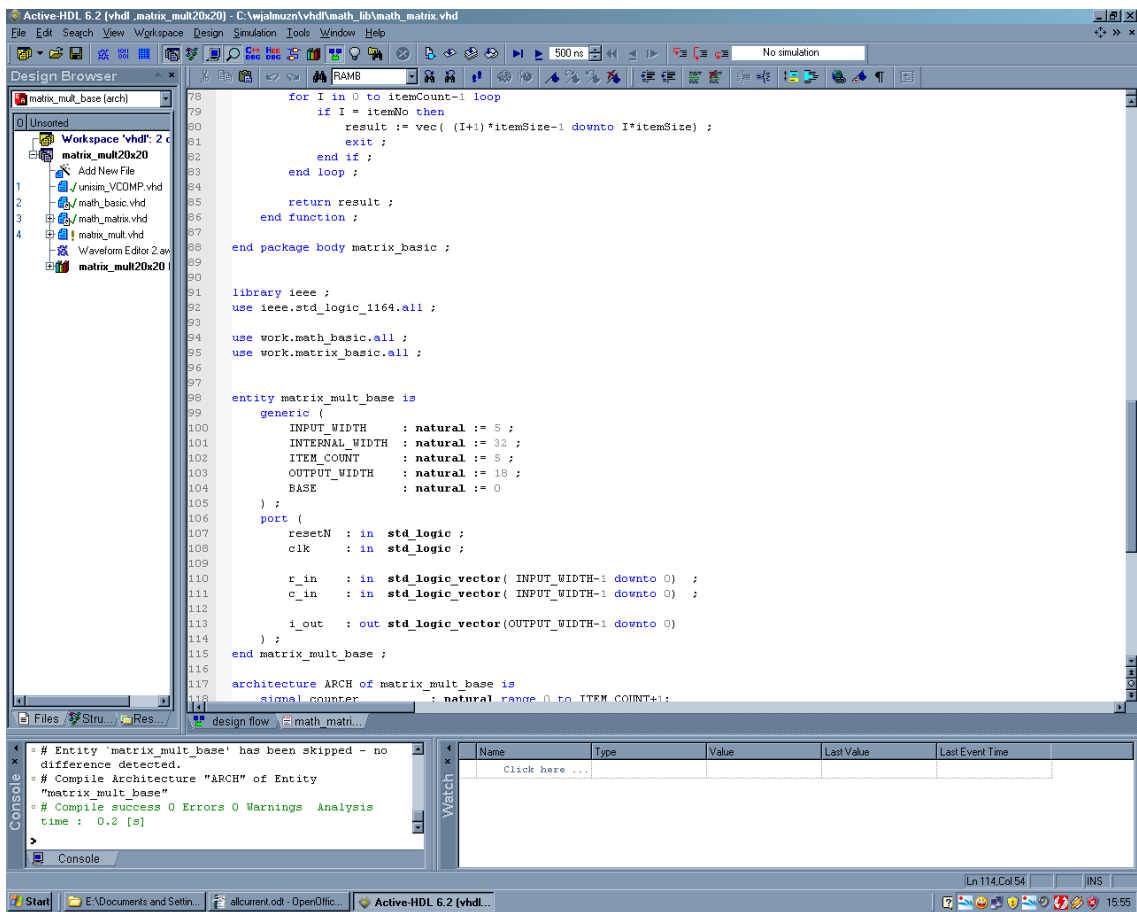


Figure 28: VHDL simulation environment

The compilation process was initiated and completed successfully. Then the input vectors were defined and simulation started. The results are shown below.

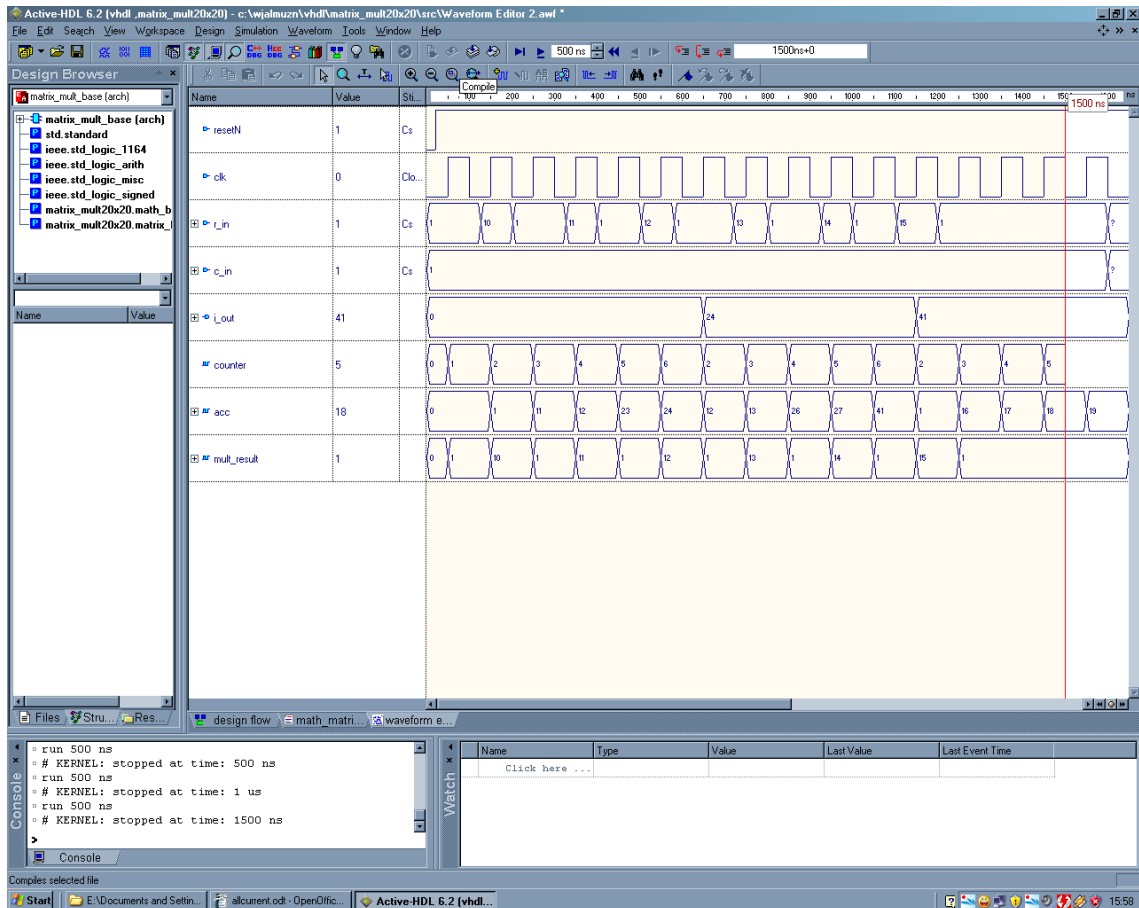


Figure 29: Simulation results

In this case the parameters `INPUT_WIDTH` and `ITEM_COUNT` were set to 5. The analysis of the simulation results shows that the component is working as planned:

The input column element was set to 1 for the whole simulation. The row element was changing during 5 clock cycles: 1,10,1,11,1. According to the chapter 3.3 the result on the output should be:  $1*1+10*1+11*1+1*1+1*1 = 24$ . This result was received after 7 clock cycles from the beginning of operation. Two additional delay cycles are caused by internal pipelined structure of the component. In the next step of verification each module was synthesized and the maximum working frequency was measured.

Moreover most of described modules were used and tested during the implementation process of the cavity detuning measurement algorithm. The final product was connected to real accelerator signals and real-time measurements were made.

This chapter presents a sample process of algorithm development and the results of measurements. The board used was the SIMCON3.1 board presented in Chapter 1.

## 5.1 Cavity detuning measurement – algorithm and implementation

During accelerator operations the resonance frequency of superconducting cavity changes. High energy field deforms the cavity's shape ( Lorentz force detuning ) and surrounding environment ( cooling system, ground motion, traffic ) causes excitation of mechanical models ( microphonics ). Frequency shift leads to cavity field errors and should be detected and compensated.

In the general transfer function for one electrical mode in superconducting cavity can be modeled as high Q bandpass described using following equation [7]:

$$\ddot{x} + 2 \omega_{\frac{1}{2}} \dot{x} + \omega_0^2 x = \omega_0 \omega_{\frac{1}{2}} y$$

The signals x and y can be represented as

$$x = x_0 e^{j\omega t} \quad y = y_0 e^{j\omega t}$$

where  $x_0$  and  $y_0$  are changing slowly ( envelope ) and exp function is changing fast. Therefore the first order envelope equation is:

$$\ddot{x}_0 - (\omega_{\frac{1}{2}} - i \Delta \omega) x_0 = \frac{y}{2i \omega_0} \quad \text{where} \quad \Delta \omega = \omega_0 - \omega_{\frac{1}{2}}$$

The translation to the polar coordinates using:

$$x = r e^{j\phi} \quad y = \rho e^{j\psi}$$

gives following equations:

$$r \dot{\phi} - r \Delta \omega = \omega_{\frac{1}{2}} \rho \sin(\psi - \phi) \quad \text{and} \quad \dot{r} + \omega_{\frac{1}{2}} r = \omega_{\frac{1}{2}} \rho \cos(\psi - \phi)$$

The first equation can be used to determine the frequency change as:

$$\Delta \omega = \frac{r \dot{\phi} - \omega_{\frac{1}{2}} \rho \sin(\psi - \phi)}{r}$$

The final mathematical formula that was implemented is:

$$\Delta \omega = \frac{-2}{\pi} \left( new_{dphase} - 2\omega_{\frac{1}{2}} \frac{|calcomplex_{forward}|}{|complex_{probe}|} \sin(\text{angle}(calcomplex_{forward}) - \text{angle}(complex_{probe})) \right)$$

$new_{dphase}$  - derivate of probe signal phase

$calcomplex_{forward}$  - complex ( IQ ) signal representing calibrated forward power

$complex_{probe}$  - complex ( IQ ) signal representing probe power

The  $complex_{forward}$  is the result of calibration between forward and reflected signals:

$$calcomplex_{forward} = Acomplex_{forward} + Bcomplex_{reflected}$$

The structure of implemented algorithm is shown on Figure 30.

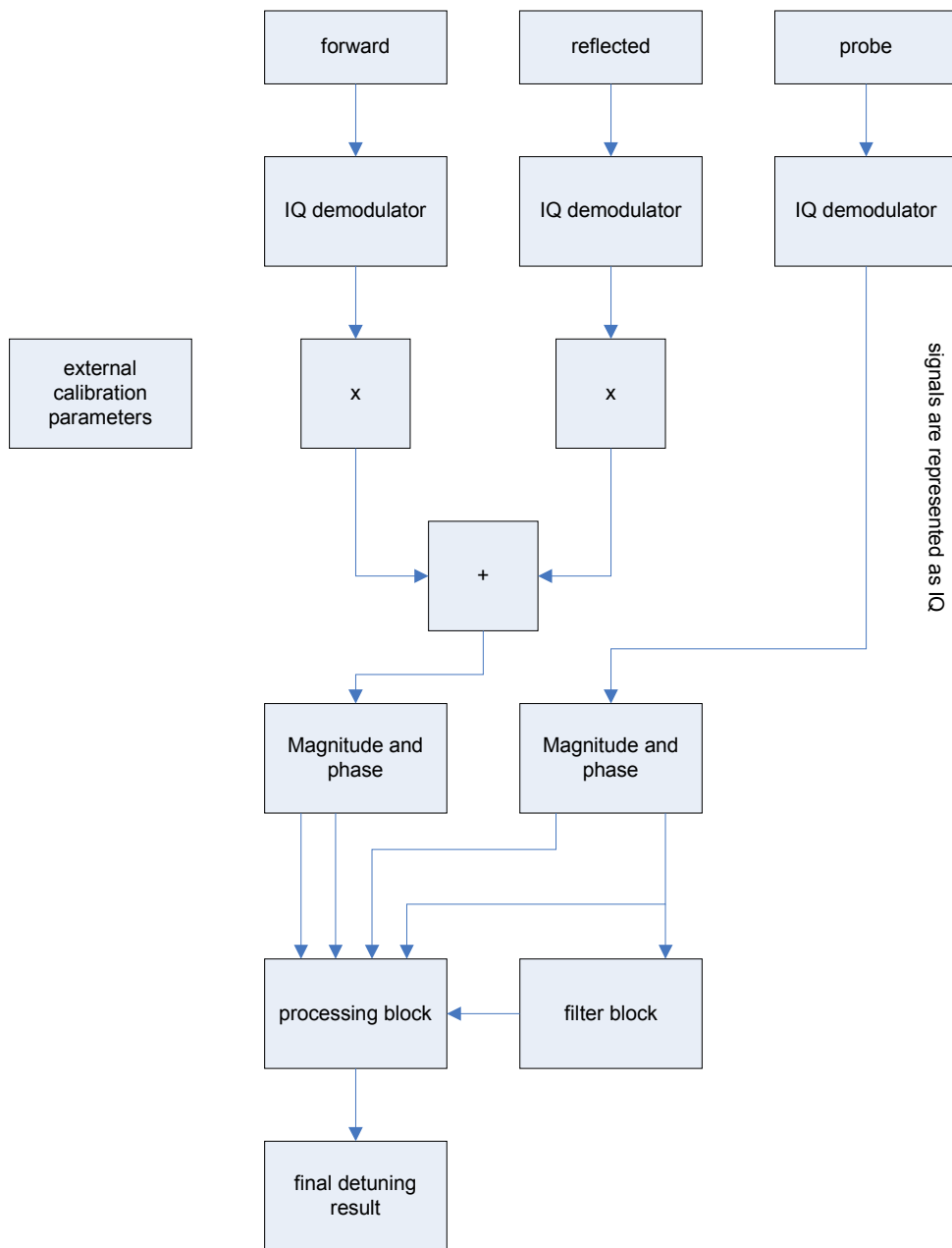


Figure 30: Structure of cavity detuning measurement implementation

The first blocks in the algorithm are IQ demodulators taken from the library. Then the signal is connected to calibration block. Two libraries can be use there: math\_basic\_signed – 8 multiplications and 4 additions/subtractions must be made or math\_complex – 2 complex multiplications and 2 additions must be made.

Signals are conected to magnitude and phase calculation block based on CORDIC algorithm. After calculations, the phase output of the probe signal is connected to derivate filter and all the signals are connected to the processing block showed on Figure 31.

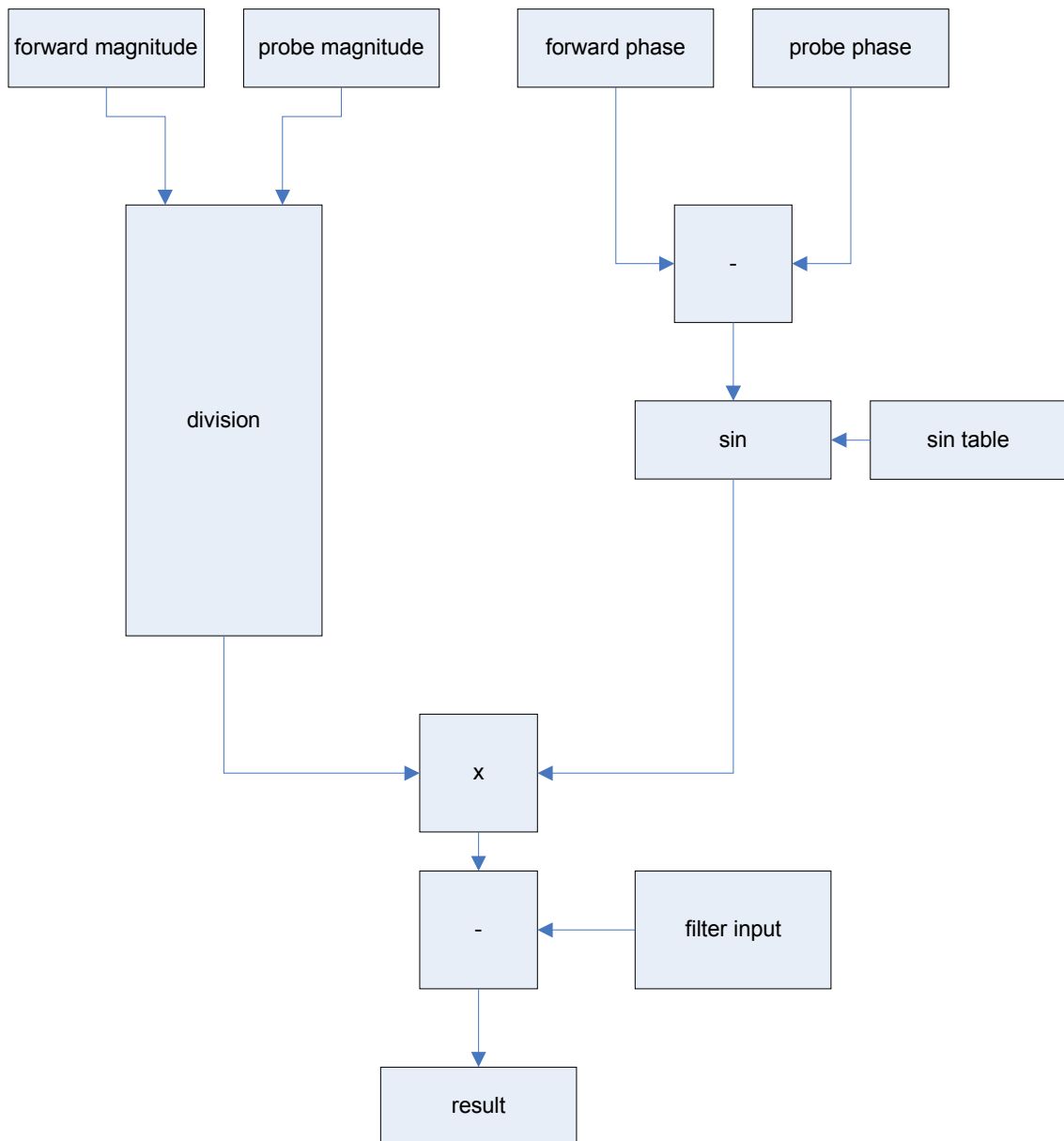


Figure 31: Structure of the processing block

Magnitudes of the probe and the forward signals are divided by the fixed point division block base on SRT modules and sine for the difference of the phases is calculated. In this case table for sine function was used – delay is time critical so CORDIC can not be used. Next divisor output and calculated sine is multiplied and result of probe phase filtering is subtracted.

The algorithm was used to evaluate the performance of the basic functional blocks:

a) IQ demodulator

The probe signal from the accelerator was sampled and connected to the IQ demodulator block. The results are shown in Figure 32

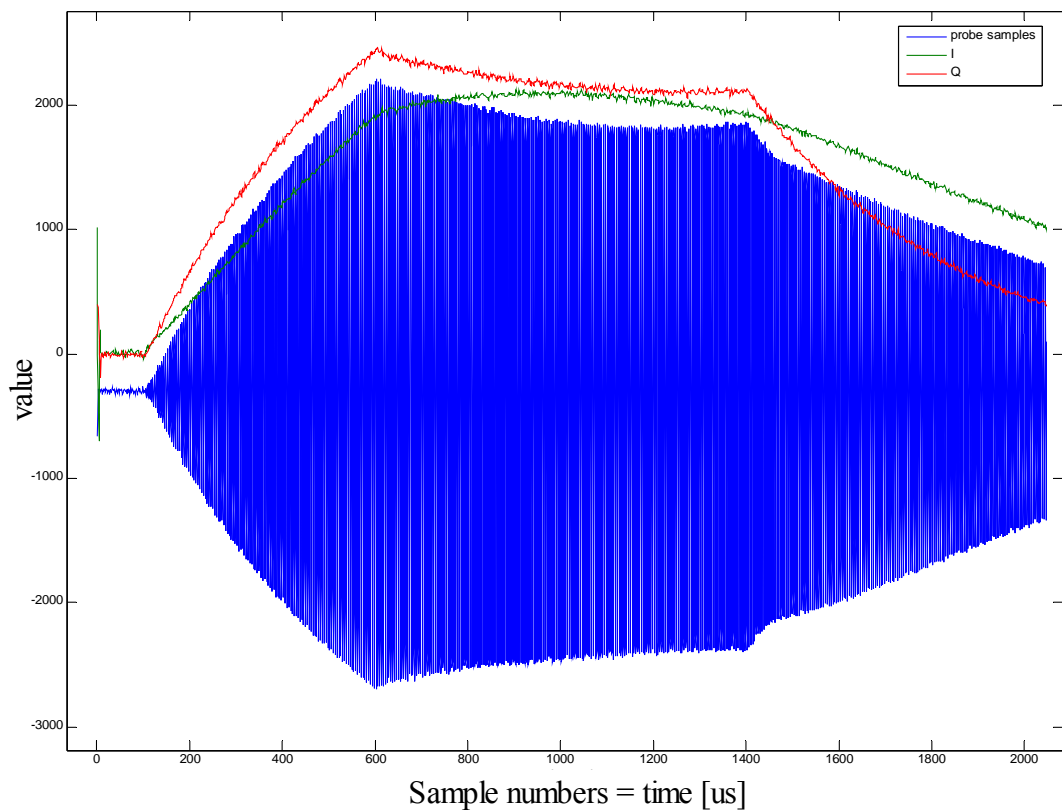
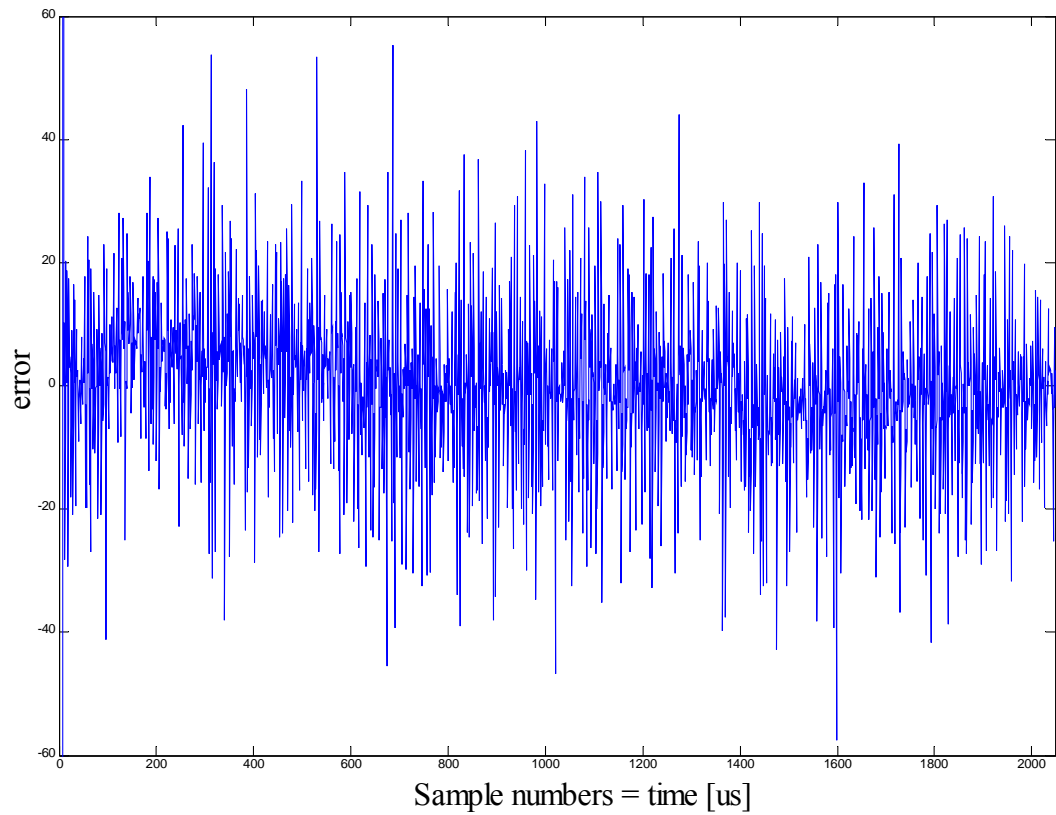


Figure 32: Probe signal with I and Q signals

The absolute error of calculations is shown on Figure 33. It is caused by fixed point representation of data in the FPGA.



*Figure 33: Absolute error of calculations*

#### b) Magnitude and phase calculations

Calculated I and Q signal was connected to the input of Magnitude and phase block. The results are shown on Figure 34. The absolute error of magnitude calculation is shown on Figure 36. In this case it is sum of quantization error caused by fixed point representation and CORDIC algorithm error.

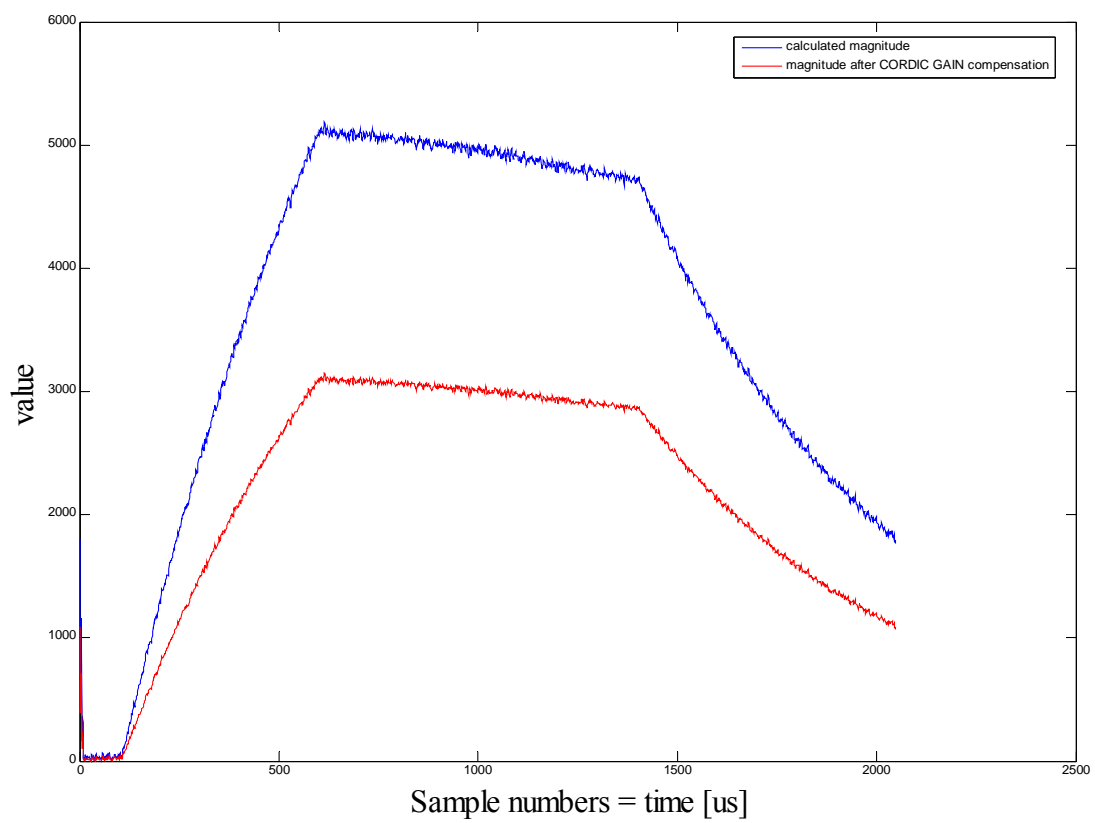


Figure 34: Magnitude result

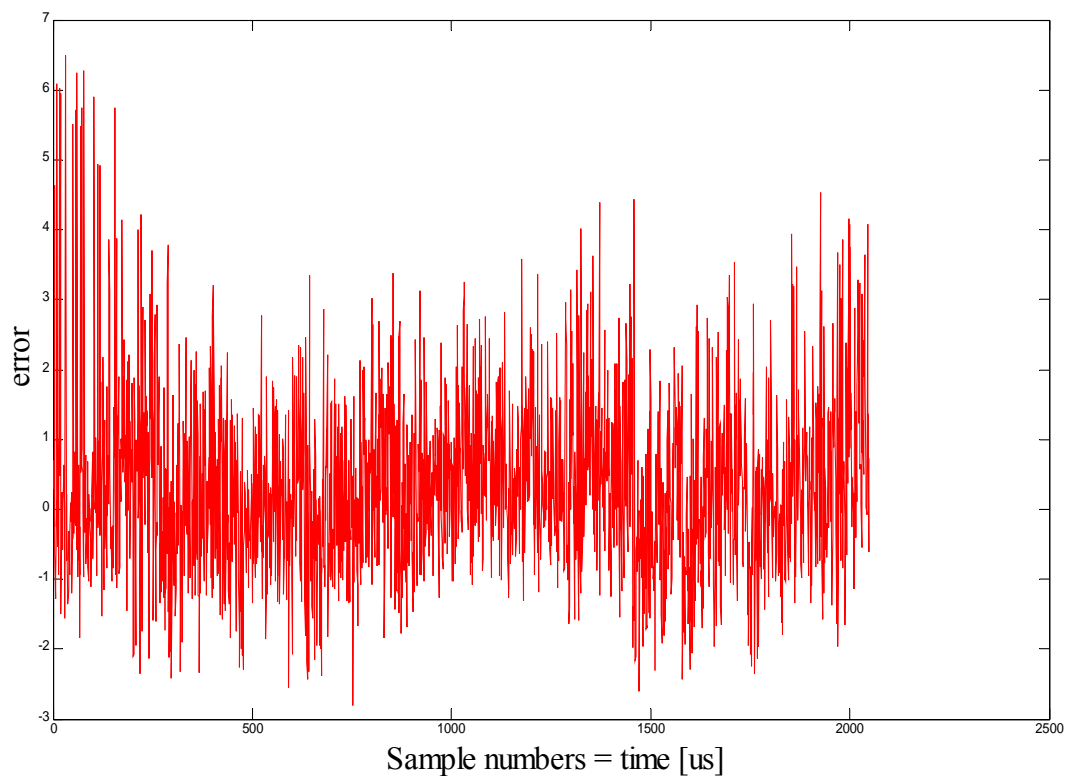
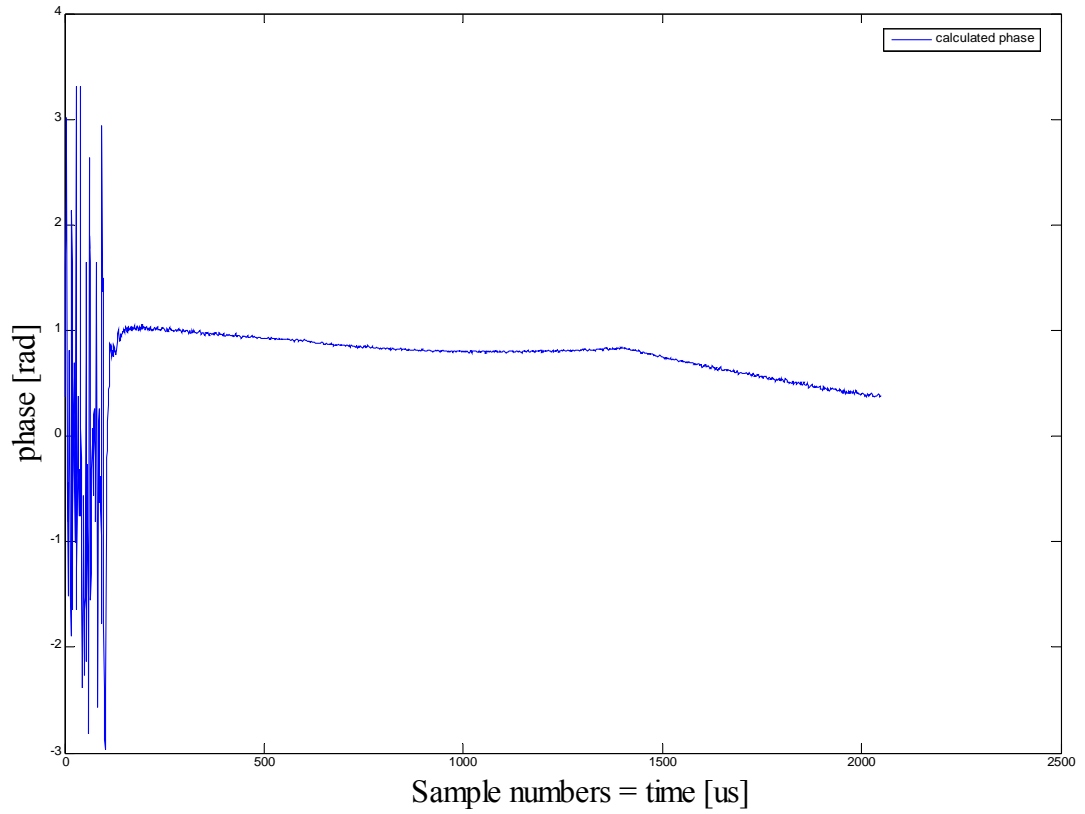


Figure 35: Absolute error of magnitude calculations

The next figure shows phase output of CORDIC block. Y axis is scaled in radians



*Figure 36: Phase calculations*

The error of the phase calculations is shown on Figure 37 Again it is sum of quantization error and CORDIC algorithm error.

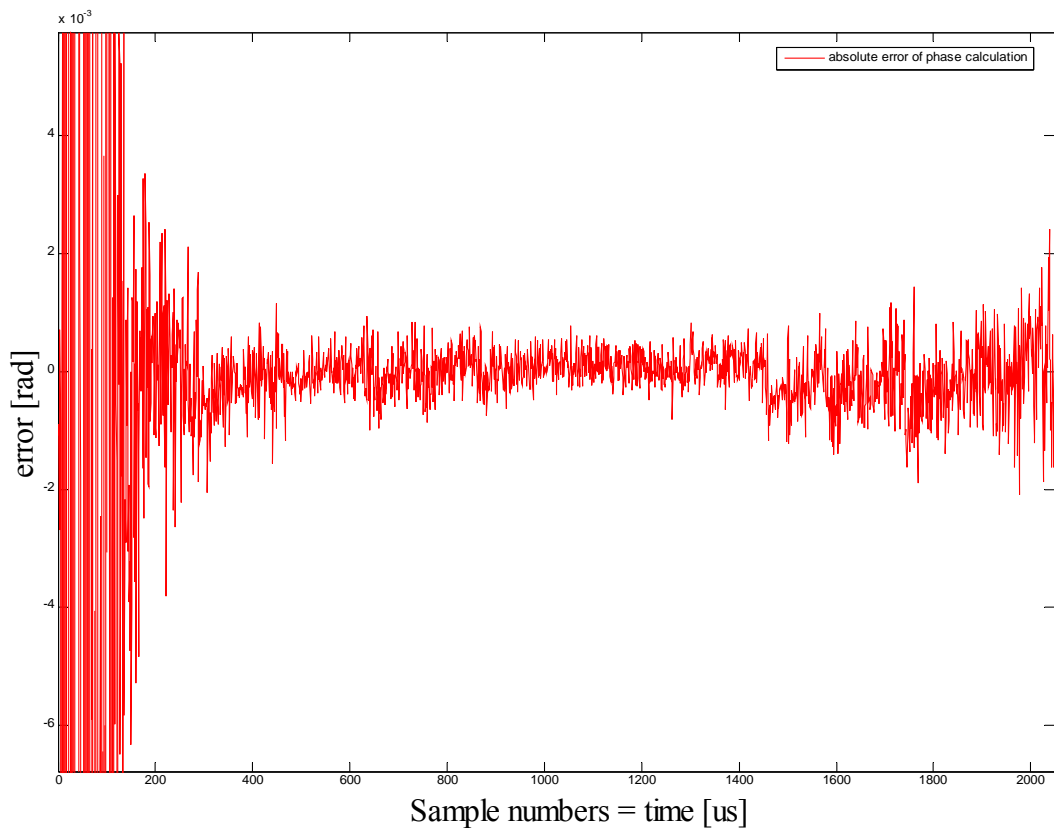


*Figure 37: Absolute error of phase calculations*

c) division block

Calculated magnitudes are delivered to the input of division block. It was configured to deliver values with 4.14 representation ( 4 bits for integer part of a number, 14 bits for fractional part ). Maximum value on division output is 7.9999. Input magnitudes are shown on Figure 38. The result of the division is shown on Figure 39.

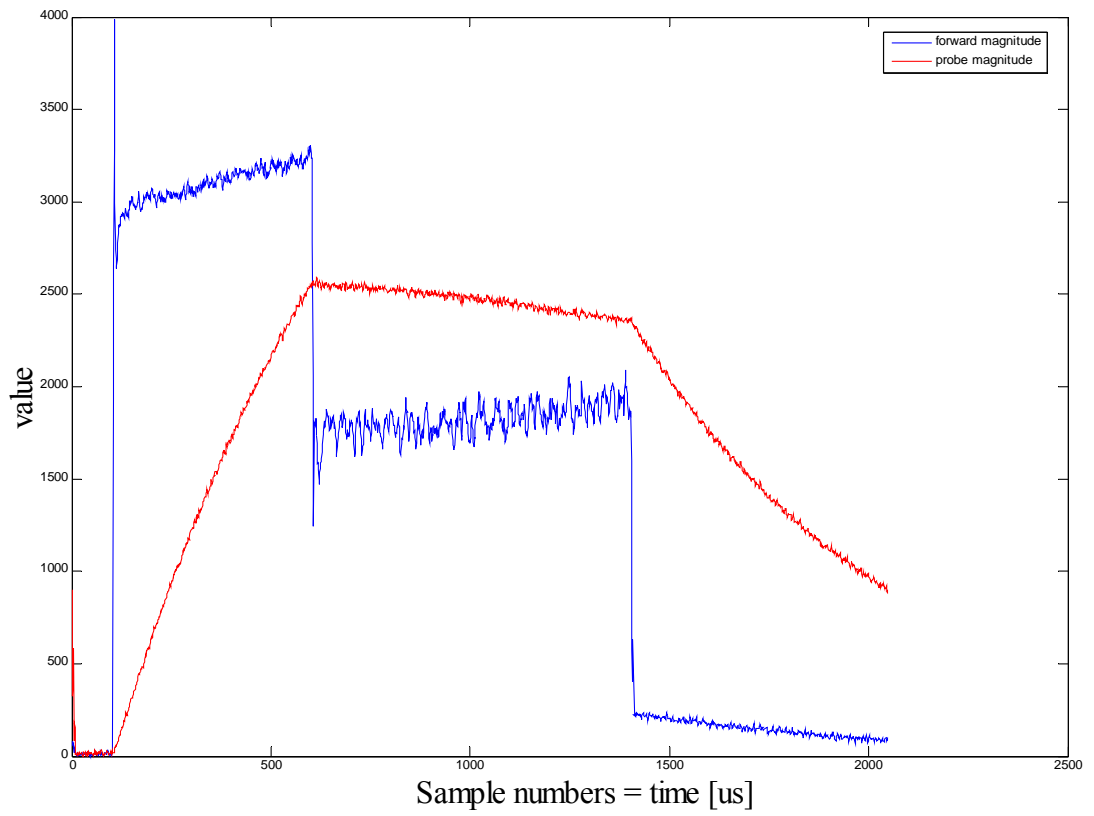


Figure 38: Inputs of the division block

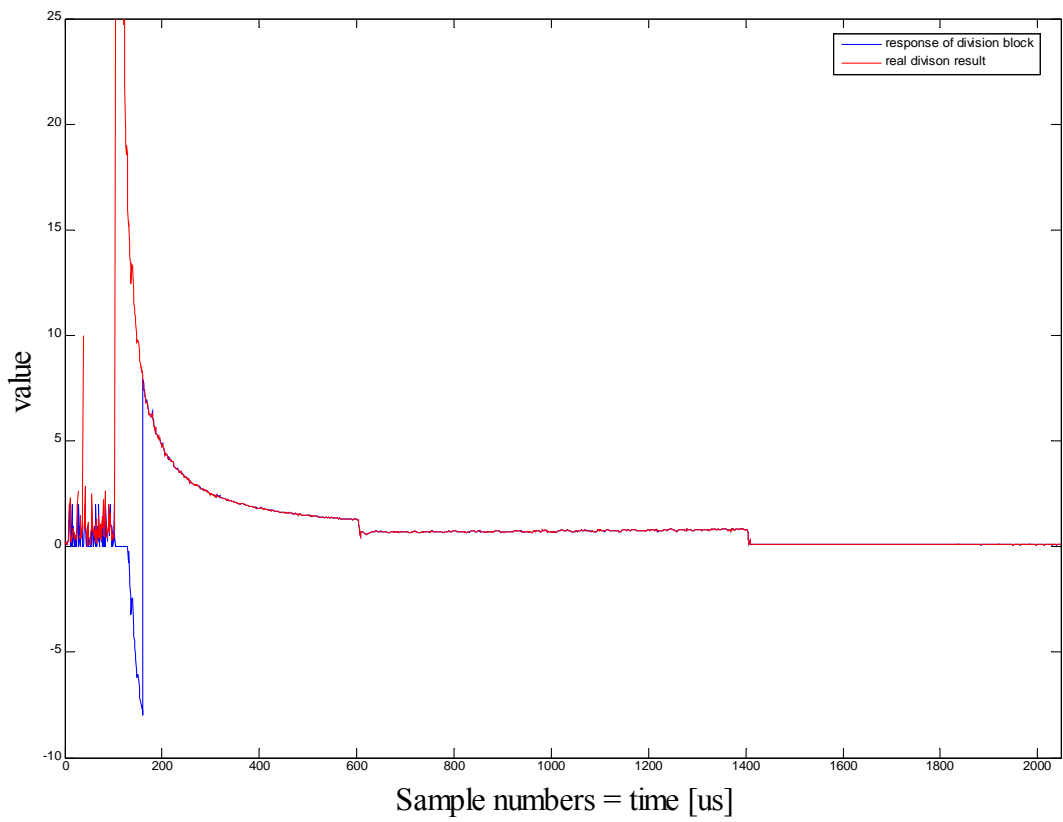
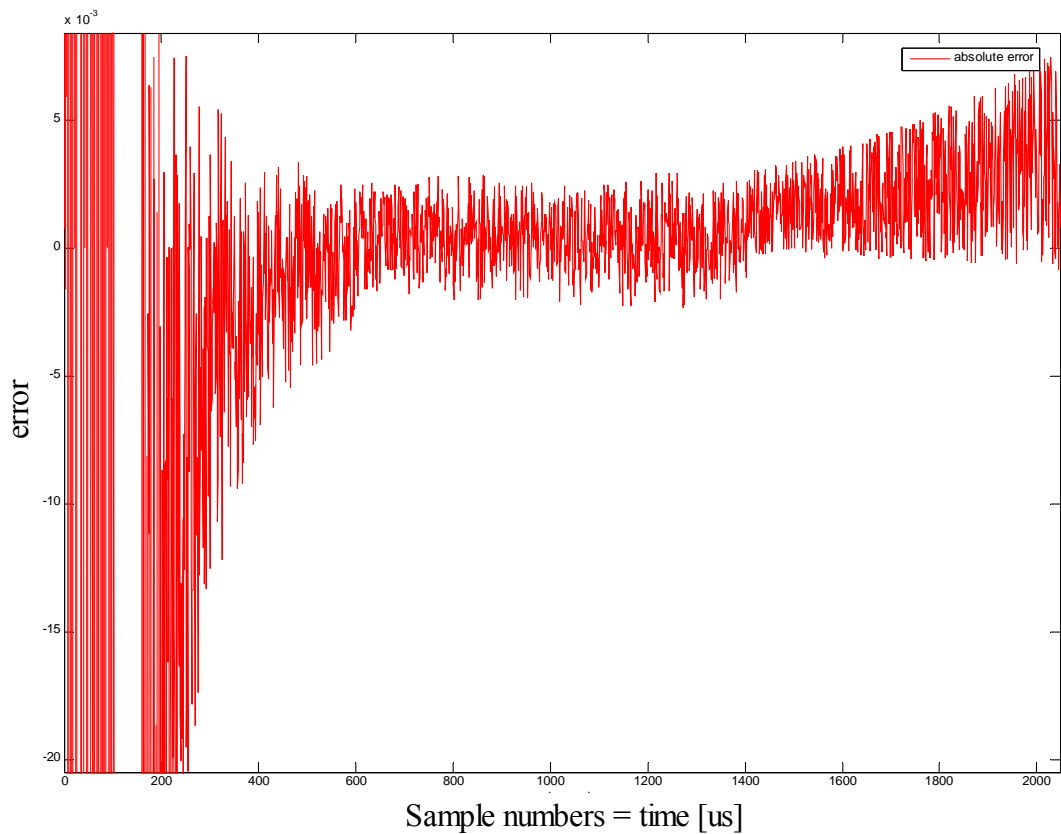


Figure 39: Division result

The division block output differs from real division result until sample 190. It is caused by chosen representation. When the real result is lower than 8, the response of the block is valid. Absolute error of calculation is shown on Figure 40. It is caused by quantization.



*Figure 40: Absolute error of division block*

SIMCON 3.1 board was configured and connected to Cavity 5 in ACC4 VUV-FEL module. Real time detuning measurements were taken. Sample results are shown of Figures 41 and 42.

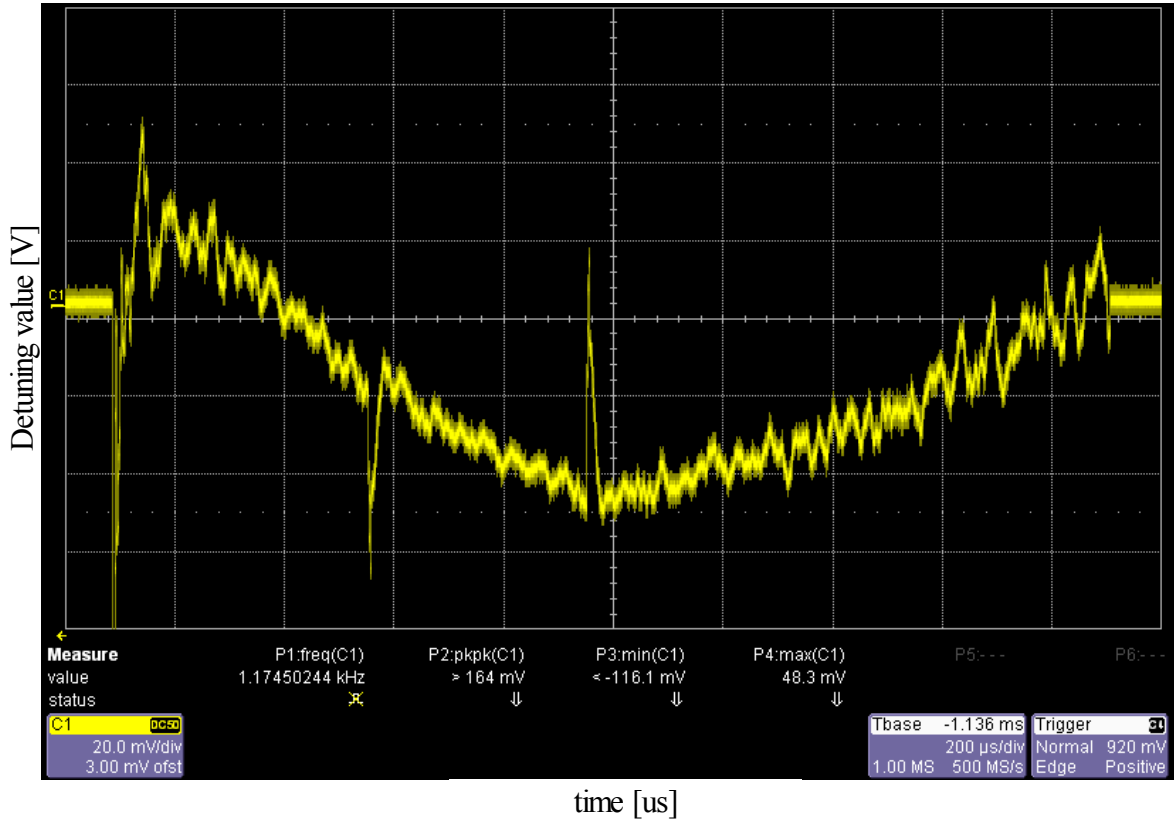


Figure 41: Detuning signal taken during measurements in VUV-FEL

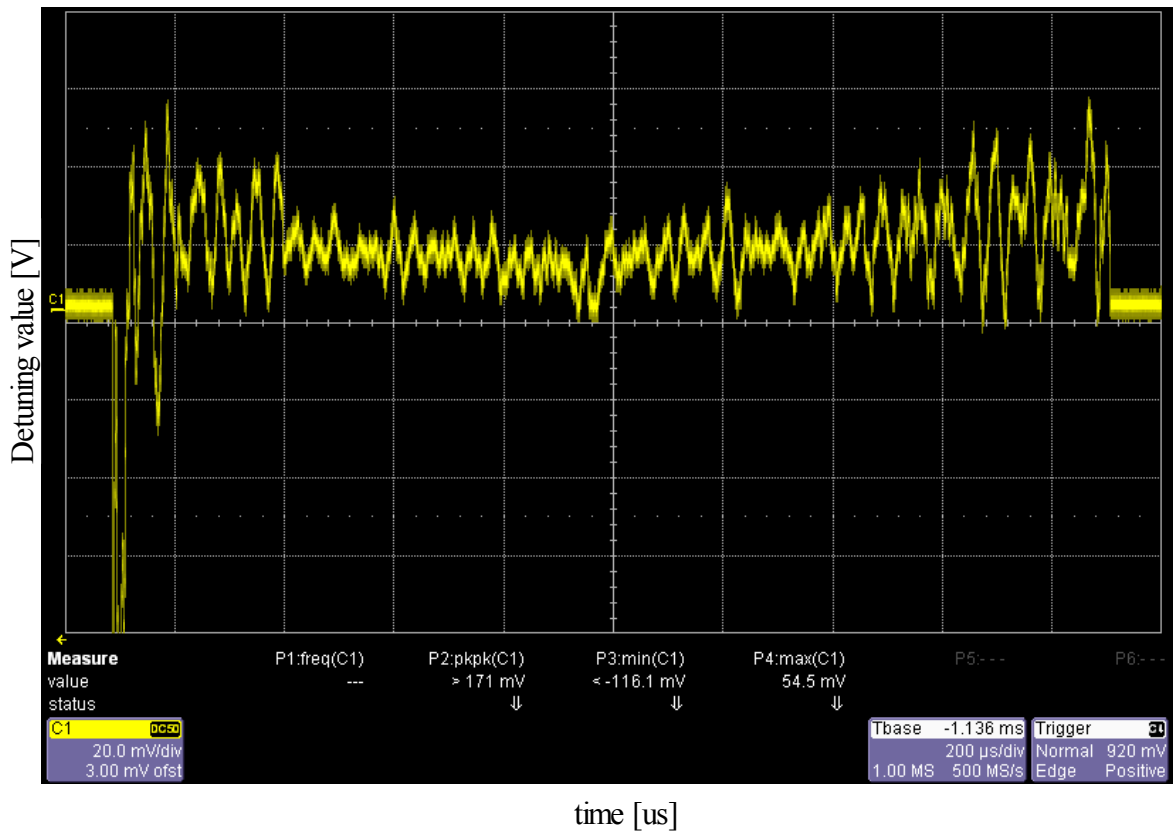


Figure 42: Detuning signal taken during measurements in VUV-FEL

## 5.2 Floating point unit tests

The OPB wrapper is used to connect floating point units to the embedded PowerPC processor. A program for the performance evaluation was written. Inputs to the operation blocks were mapped to the address space. PowerPC performed following tasks:

1. 10000000 floating point add/subtracts were executed using software emulation provided by Xilinx PPC library. Mean time of single operation was measured.
2. The same task was performed but using hardware cores
3. The process was repeated for multiplication and division

The results from serial console on PPC are shown below:

```
MULTIPLICATION STATS

software emulation
single operation: 2404.072998
hardware support
single operation: 289.000000

ADD/SUB STATS

software emulation
single operation: 2347.683838
hardware support
single operation: 286.000000

DIV STATS

software emulation
single operation: 4824.583496
hardware support
single operation: 407.000000
```

Table 7 summarizes the results

	sum/sub	mult	div
software	2347.683838	2404.072998	4824.583496
hardware	286.000000	289.000000	407.000000
acceleration	8.2	8.31	11.85

Table 7: Floating point core evaluation

The times are shown in processor clock cycles ( PPC frequency is 300MHz, OPB bus frequency is 100MHz). Most of hardware latency is caused by input/output operation delays in PPC system.

### 5.3 Matrix multiplication tests

To evaluate performance of matrix\_mult\_base module, the following structure for 20x20 matrix multiplication was implemented. It allows to upload matrix data into 2 input memories using the communication interface ( in this case Internal Interface ). Multiplication is executed and result matrix is stored in output memory.

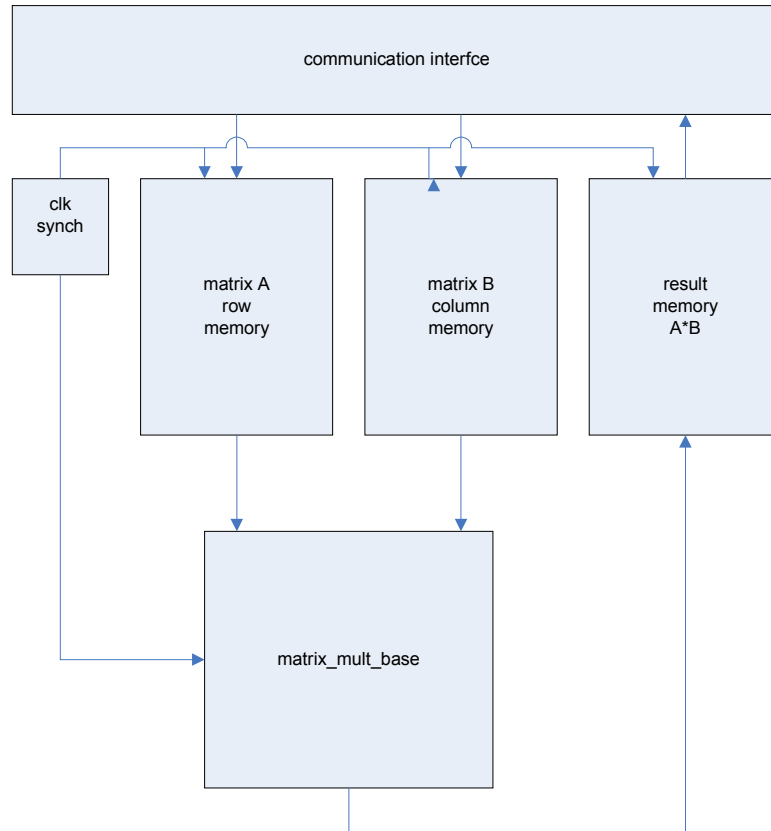


Figure 43: Implemented matrix multiplication

The CLK/SYNCH block provides the clocking signal for multiplication unit and memories. Moreover it controls addresses delivered to the memories to provide synchronization between rows and columns. The configuration of the multiplication unit is following:

```
INPUT_WIDTH = 18   INTERNAL_WIDTH = 24
OUTPUT_WIDTH= 18   ITEM_COUNT      = 20   BASE=0
```

Presented unit was implemented using Virtex 2 Pro XC2VP30 chip. Following performance was achieved.

Speed grade	LUTs	FlipFlops	18x18 mult	Block RAM	Maximum freq.
-5	128	57	1	3	90 MHz
-6	128	57	1	3	100 MHz
-7	128	57	1	3	115 MHz

*Table 8: Performance and resource usage of matrix multiplication unit*

Resource usage does not include resources used by communication interface. The calculation of one element takes 20 clock cycles. The whole result matrix with 400 element takes 8000 clock cycles. Additional 2 clock cycles are needed. The final result is known after 8002 clock cycles. For -6 speed grade when the clock period is 10ns it takes 80020 ns ( 80,02 us ). Table 9 shows multiplication time for a different number of used hardware multipliers

Number of multipliers	Operation time [us]
1	80
2	40
4	20
8	10

*Table 9: Matrix 20x20 multiplication time*

## 6. Summary and conclusions

Presented library is now in testing stage. Initial tests and first algorithm implementations showed that the base concept is correct and can be used in future development. The following group of the system were implemented and tested – they are accessible for end-user:

- input modules - ( they include IQ demodulator and Magnitude and phase calculations ) which provide easy conversion of raw data into necessary representation. These modules execute input stages of many algorithms and provide data for core modules which execute main calculations
- core modules – they execute specific functionality such as division, sin/cos calculation, data filtering. They can be connected to each other or to input modules to create structure necessary for specific algorithm implementation.
- embedded systems support – they provide interface to the embedded system, which allows to connect and map any other module into embedded system's address space and floating point module to provide floating point arithmetical operations. Future tests with embedded DOOCS servers that need fast floating point operations may show the real value of these modules
- low level modules ( they include libraries such as `math_basic_signed`, `math_complex`, etc. ) which allow to implement any functionality which is not included into other modules. They implement basic concepts of mathematical library such as saturation arithmetic, complex numbers operation and so on. User can easily implement his own modules without special considerations

All blocks were optimized to provide reasonable choice between performance and resource usage according to possibilities in target accelerator environment, but in future versions of this library they can be further optimized to fit to the changing needs of the

system. Performance will change together with FPGA market changes and some resource constraints may be dropped ( when the prices of FPGA chips decrease and available resources increase ). Moreover the functional blocks written by the author or end-users may be added to fit the needs of other groups and environments. The proposed solution provides easy and fast way to implement algorithms, so it will easily be integrated with existing systems. Architecture of the library is open so, in future, components will be upgraded and new elements added.

## References

- [1] T. Czarski, K. Pozniak, R. Romaniuk S. Simrock: TESLA Cavity Modeling and Digital Implementation with FPGA Technology Solution for Control System Purpose. TESLA internal note 2003-28.
- [2] W. Giergusiewicz, W. Koprek, W. Jalmuzna, K. T. Pozniak, R. S. Romaniuk FPGA Based, DSP Integrated, 8-Channel SIMCON, ver. 3.0. Initial Results for 8-Channel Algorithm. Tesla internal note 2005-14.
- [3] T. Czarski, R. S. Romaniuk, K. T. Pozniak, S. Simrock: Cavity control system: optimization methods for single cavity driving and envelope detection, Proceedings of SPIE, Bellingham, WA, USA, Vol. 5484, 2004, pp. 99-110.
- [4] Krzysztof T. Pozniak, Ryszard S. Romaniuk Modular and Reconfigurable Common PCB Platform of FPGA Based LLRF Control System for TESLA Test Facility, TESLA Report 2005-04.
- [5] W.M. Zabolotny, T. Czarski, T. Jezynski, K.T. Pozniak, P. Rutkowski, R.S. Romaniuk, K. Bunkowski, FPGA Based Cavity Simulator for TESLA Test Facility, TESLA Report 2003-22.
- [6] FPGA and Optical Network Based LLRF Distributed Control System for TESLA-XFEL Linear Accelerator - Krzysztof T. Pozniak, Ryszard S. Romaniuk, Tomasz Czarski, Wojciech Giergusiewicz, Wojciech Jalmuzna, Krzysztof Olowski, Karol Perkuszewski, Jerzy Zielinski - Institute of Electronic Systems, Warsaw University of Technology; Stefan Simrock – Tesla internal note 2004-09
- [7] Thomas Schilcher , Vector Sum Control of Pulsed Accelerating Fields in Lorentz Force Detuned Superconducting Cavities

- [8] Waldemar Koprek, Pawel Kaleta, Jaroslaw Szewinski, Krzysztof T. Pozniak, Ryszard S. Romaniuk: Software Layer for SIMCON ver. 1.1., FPGA based TESLA Cavity Control System; USER'S MANUAL. TESLA internal note 2005-05.
- [9] S.K. T. Pozniak, M. Bartoszek, M. Pietrusinski, Internal interface for RPC muon trigger electronics at CMS experiment, Proceedings of SPIE, Bellingham, WA, USA, Vol. 5484, 2004, pp. 269-282.
- [10] Krzysztof Pozniak - INTERNAL INTERFACE, I/O Communication with FPGA Circuits and Hardware Description Standard for Applications in HEP and FEL Electronics ver. 1.0 - Tesla internal note 2005-22.
- [11] Ray Andraka - A survey of CORDIC algorithms for FPGA based computers
- [12] David L. Harris, Stuart F. Oberman, and Mark A. Horowitz- SRT Division Architectures and Implementations
- [13] J. Szabat in Podstawy teorii sygnałów, WKŁ 2003
- [14] T. P. Zieliński Od teorii do cyfrowego przetwarzania sygnałów, Wydawnictwo AGH 2002.
- [15] [www.desy.de](http://www.desy.de) – DESY homepage.
- [16] [tesla.desy.de](http://tesla.desy.de) – TESLA homepage.
- [17] [www.xilinx.com](http://www.xilinx.com) – homepage of manufacturer of FPGA chips
- [18] [www.altera.com](http://www.altera.com) - homepage of manufacturer of FPGA chips
- [19] [www.opencores.org](http://www.opencores.org) – FPGA resources webpage
- [20] [www.ieee.org](http://www.ieee.org) – IEEE homepage

## **Acknowledgments**

Author would like to thank everyone, who helped him during realisation of this M.Sc.Thesis. Especially: Ph.D. Ryszard Romaniuk, Ph.D. Krzysztof Pozniak from Warsaw University of Technology and Ph.D. Stefan Simrock and Alexander Brandt from Deutches Electronen Synchrotron (Hamburg) for their supervision and opportunity for projects to be started.

Author would like to thank ALDEC company for the opportunity to use their ActiveHDL software for FPGA simulations.

Author would like to thank DESY Directorate, especially dr. Alexander Gamp, for providing superb technical, financial and social conditions, for the TESLA LLRF Group and the ELHEP Warsaw Group, to perform the work described in this paper.

## **7. Appendixes**